HZB Helmholtz Zentrum Berlin

SwedNESS: Real-Space Neutron Imaging

Scattering and magnetic contrast

Nikolay Kardjilov

Particle-wave duality

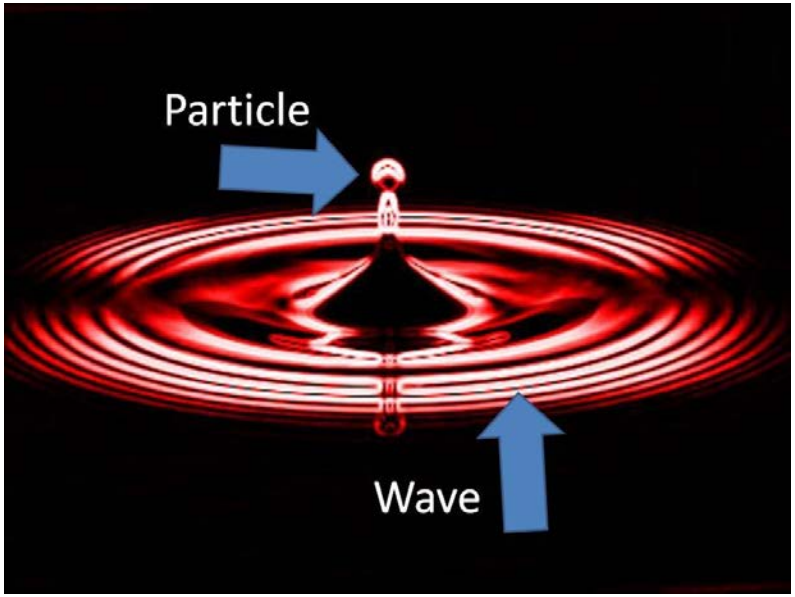

- de-Broglie wavelength: $\lambda = \frac{2\pi\hbar}{mv},$
- Wave number: $k = 2\pi/\lambda, \quad \mathbf{k} = \frac{m_{\mathrm{n}}\mathbf{v}}{\hbar}.$
- Momentum: $p = \hbar k$
- Momentum operator: $\hat{\mathbf{p}} = -i\hbar\nabla$
- Kinetic energy: $E = \frac{\hbar^2 k^2}{2m_{\mathrm{n}}},$

Wave–particle duality is the concept in quantum mechanics that every particle or quantum entity may be partly described in terms not only of particles, but also of waves.
Hence the material particles like neutrons, also have wave properties such as wavelength and frequency.

Phase and dark-field contrast

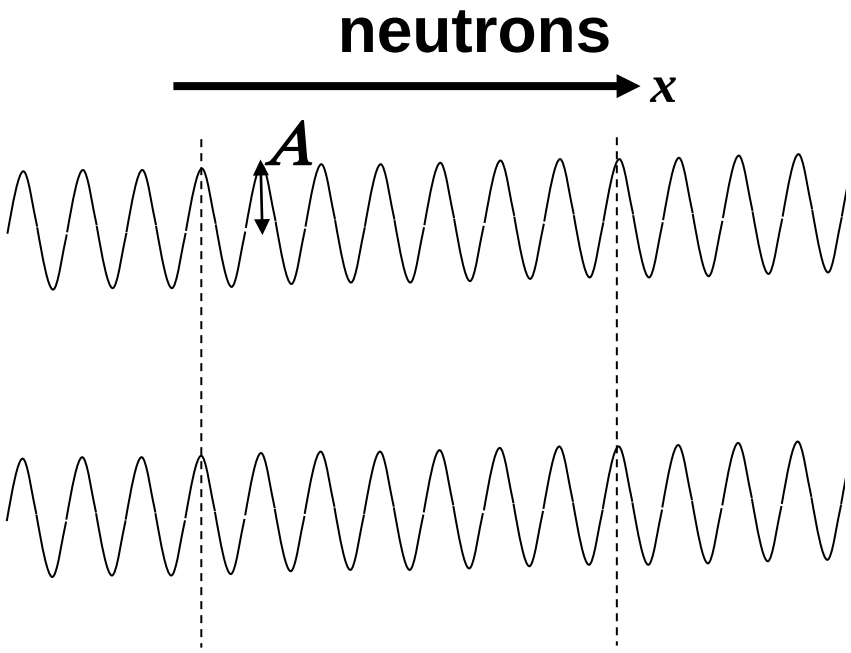

$$\Psi_{before} = A \cdot e^{-i(\omega t - kx)}$$

wave function

The wave nature of the neutron can also be utilized for phase contrast imaging. For this purpose, a coherent beam of neutrons is needed in order to describe wave propagation through a sample.

Phase and dark-field contrast

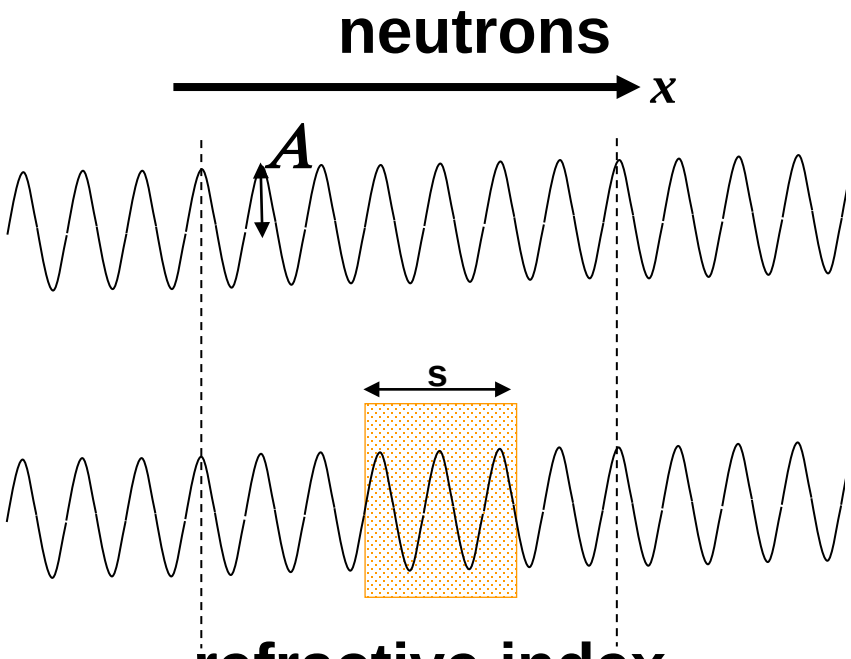

$$\Psi_{before} = A \cdot e^{-i(\omega t - kx)}$$

wave function

As the coherent wave front interacts with the sample, the refractive index of the material describes the change of the amplitude of the wave (absorption) or the shift of the phase (refraction).

Phase and dark-field contrast

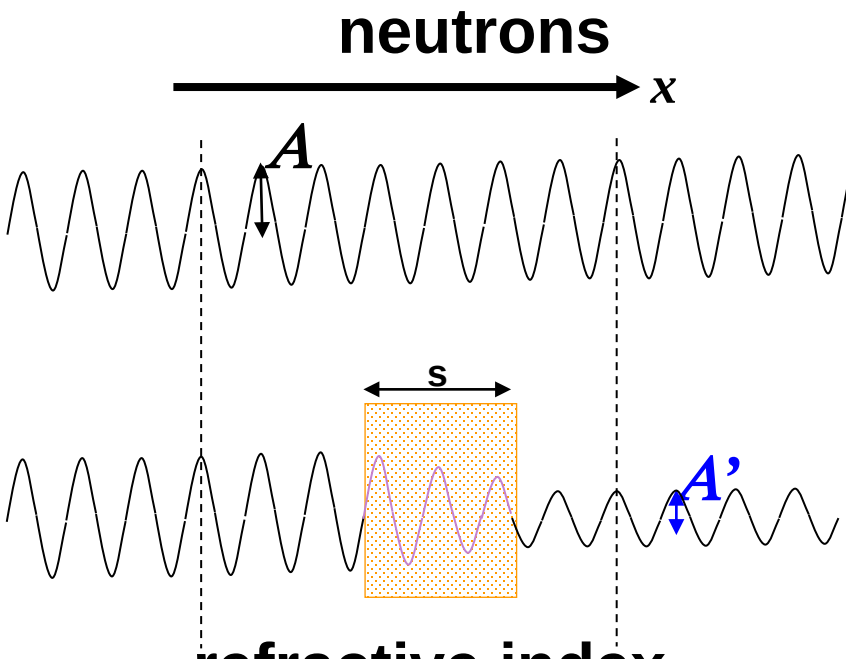

$$\Psi_{before} = A \cdot e^{-i(\omega t - kx)}$$

wave function

As the coherent wave front interacts with the sample, the refractive index of the material describes the change of the amplitude of the wave (absorption) or the shift of the phase (refraction).

Phase and dark-field contrast

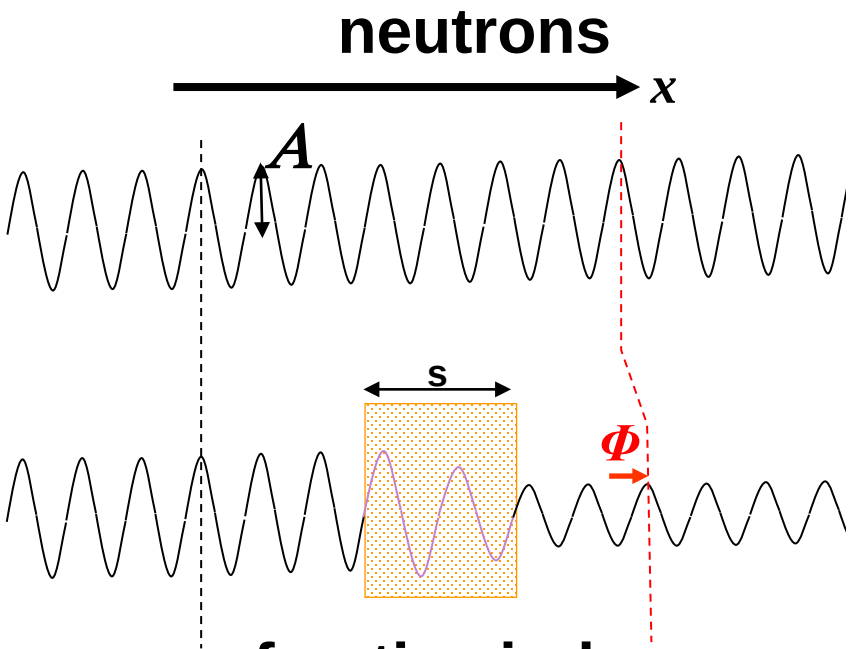

$$\Psi_{before} = A \cdot e^{-i(\omega t - kx)}$$

wave function

As the coherent wave front interacts with the sample, the refractive index of the material describes the change of the amplitude of the wave (absorption) or the shift of the phase (refraction).

Phase and dark-field contrast

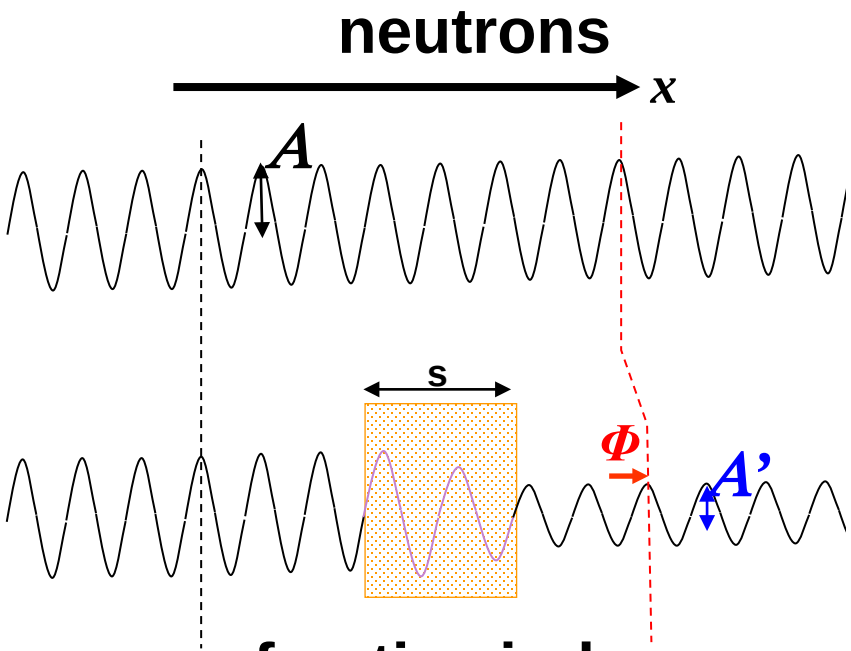

$$\Psi_{before} = A \cdot e^{-i(\omega t - kx)}$$

wave function

$$\Psi_{after} = \underbrace{e^{-i(2\pi\delta/\lambda)s}}_{\Phi} \cdot \underbrace{e^{-(2\pi\beta/\lambda)s}}_{A'/A} \cdot \Psi_{before}$$

As the coherent wave front interacts with the sample, the refractive index of the material describes the change of the amplitude of the wave (absorption) or the shift of the phase (refraction).

Phase and dark-field contrast

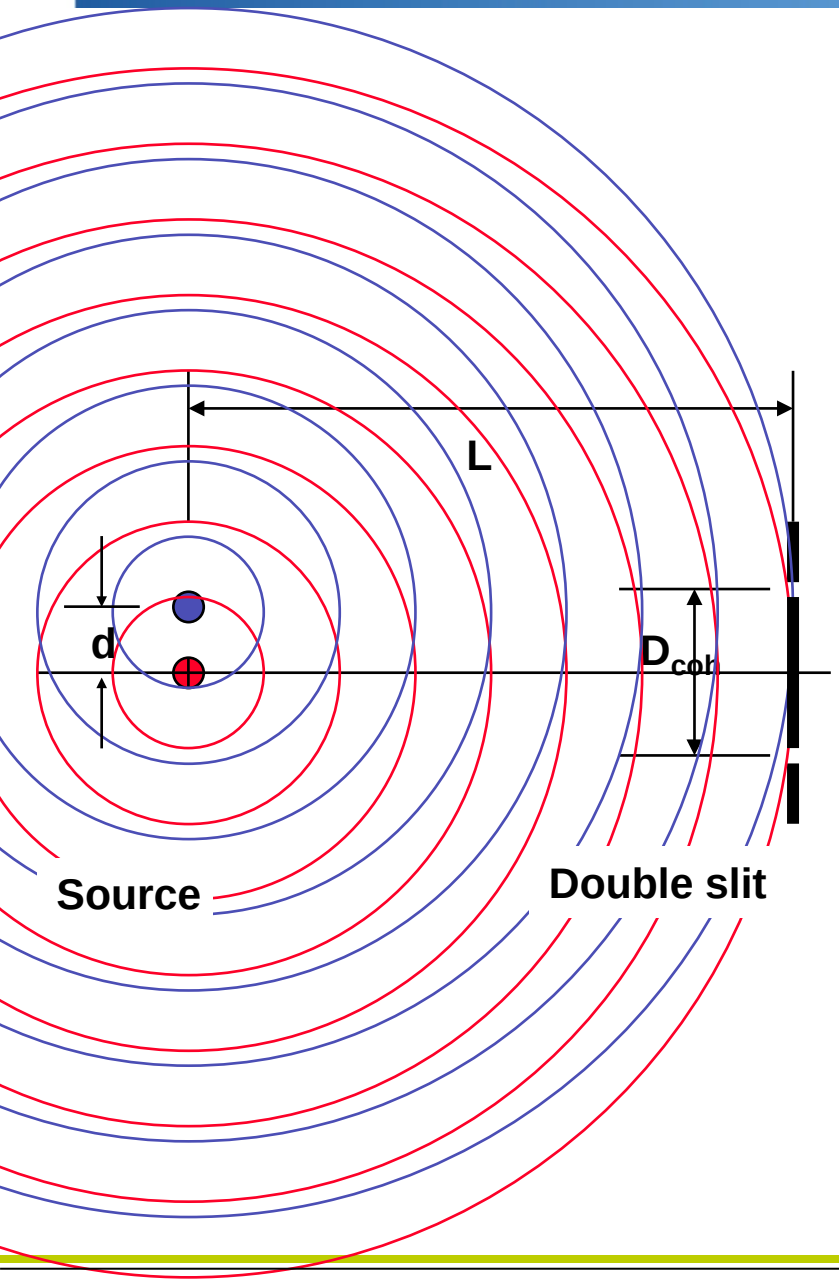

In case of a point-like source as defined by a small pinhole (*d*), the emanating spherical wave exhibits a high degree of transverse spatial coherence in area D_{coh} even when a polychromatic source is used.

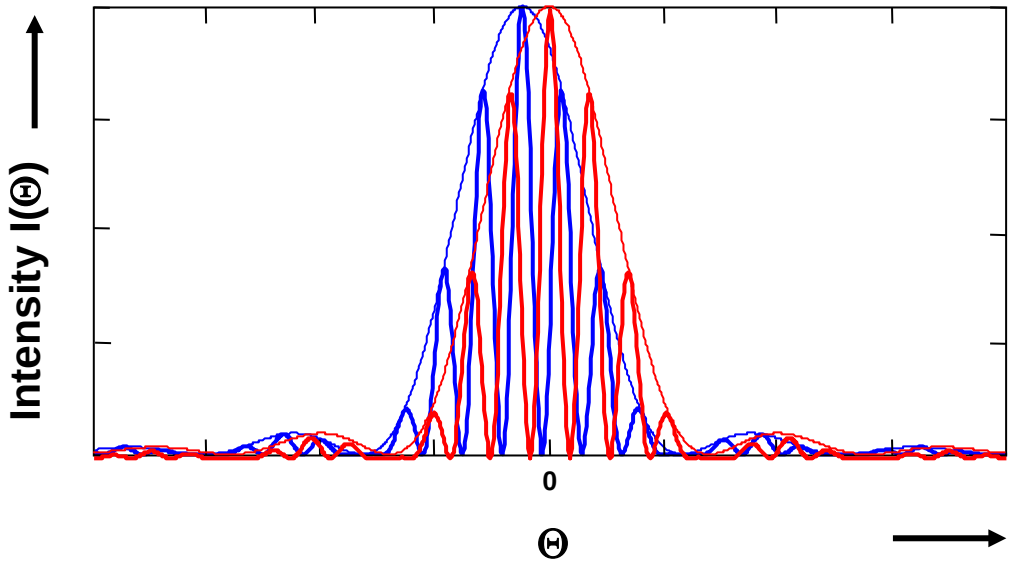

Phase and dark-field contrast

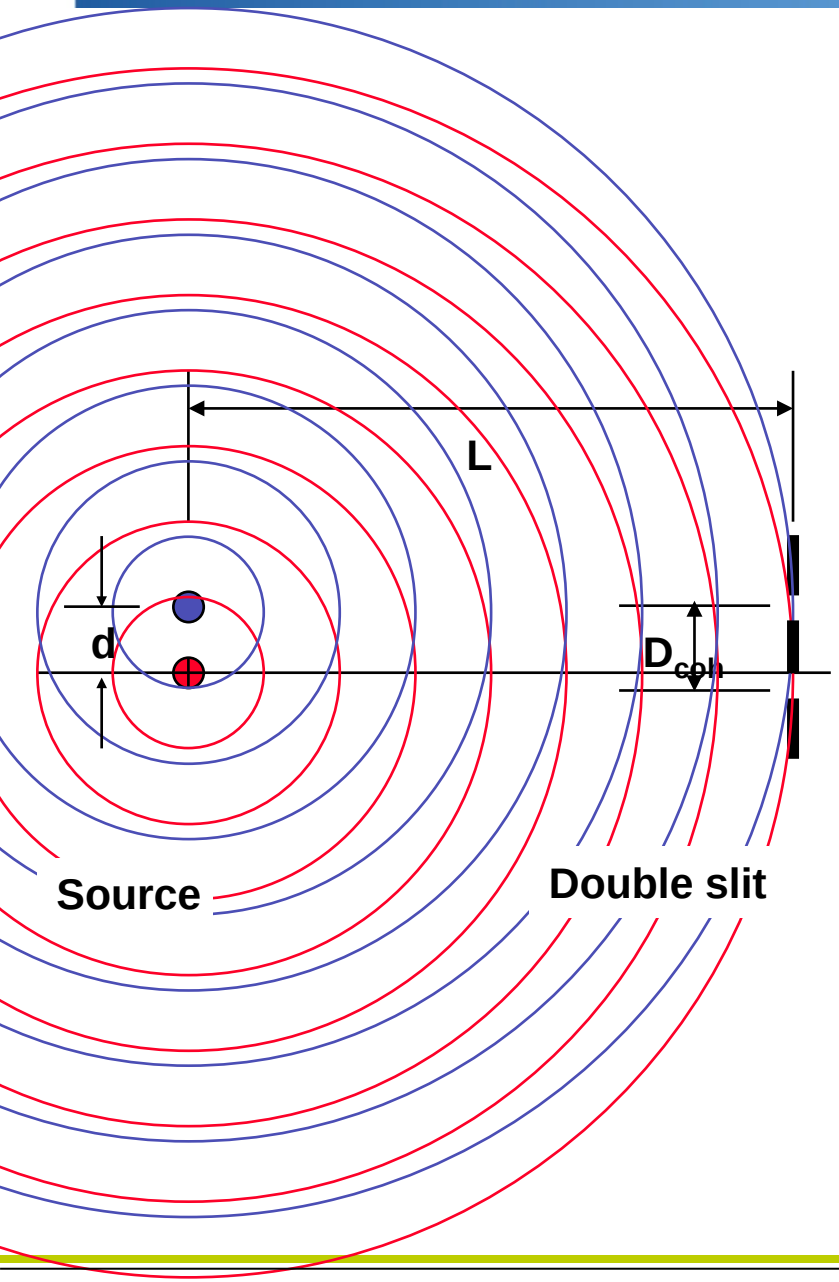

Spatial coherence

D_{coh} ~ L λ / s

Example:	**Thermal neutrons**
λ=0.2nm	**Wavelength**
L=5m	**Distance**
s=1mm	**Source size**
⇒ D_{coh} ~ 1µm	**Coherence length**

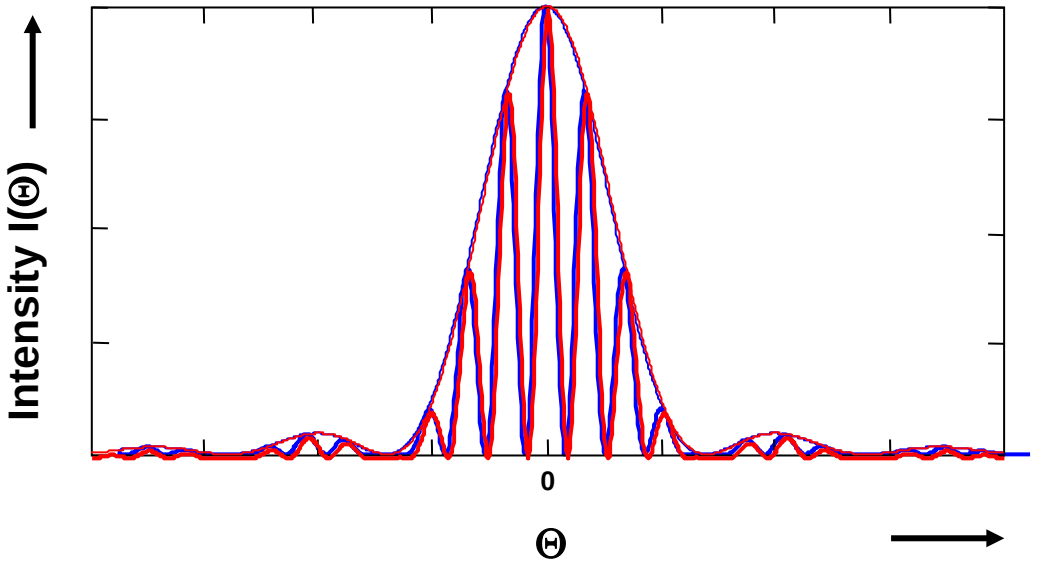

Spatial coherence

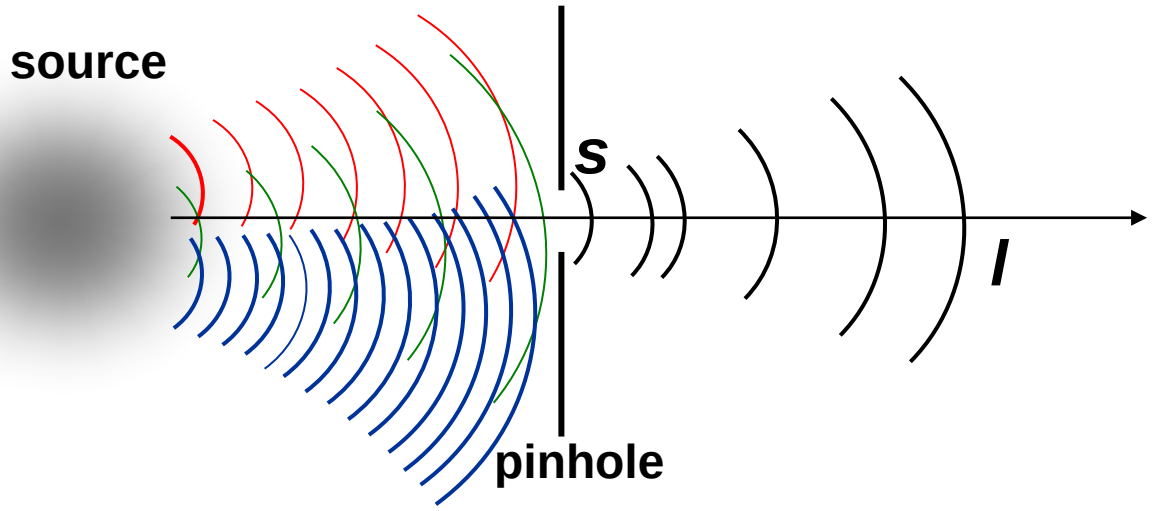

The lateral coherence length is $d = \lambda l/s$.

Thus high spatial coherence may be achieved by using a source of small effective size or by observing the beam at a large distance from the source.

Phase and dark-field contrast

Connection between phase and intensity variation

The surfaces where $\varphi(r)$ is constant are represented as wavefronts.

Normal to the wavefront:

$$\mathbf{s}(x,y,z) \approx \left(-\frac{\partial\varphi}{\partial x}, -\frac{\partial\varphi}{\partial y}, k\right)$$

Angular deviation of the normal:

$$\Delta\alpha \approx \frac{1}{k}\left|\nabla_{\perp}\varphi(x,y,z)\right|$$

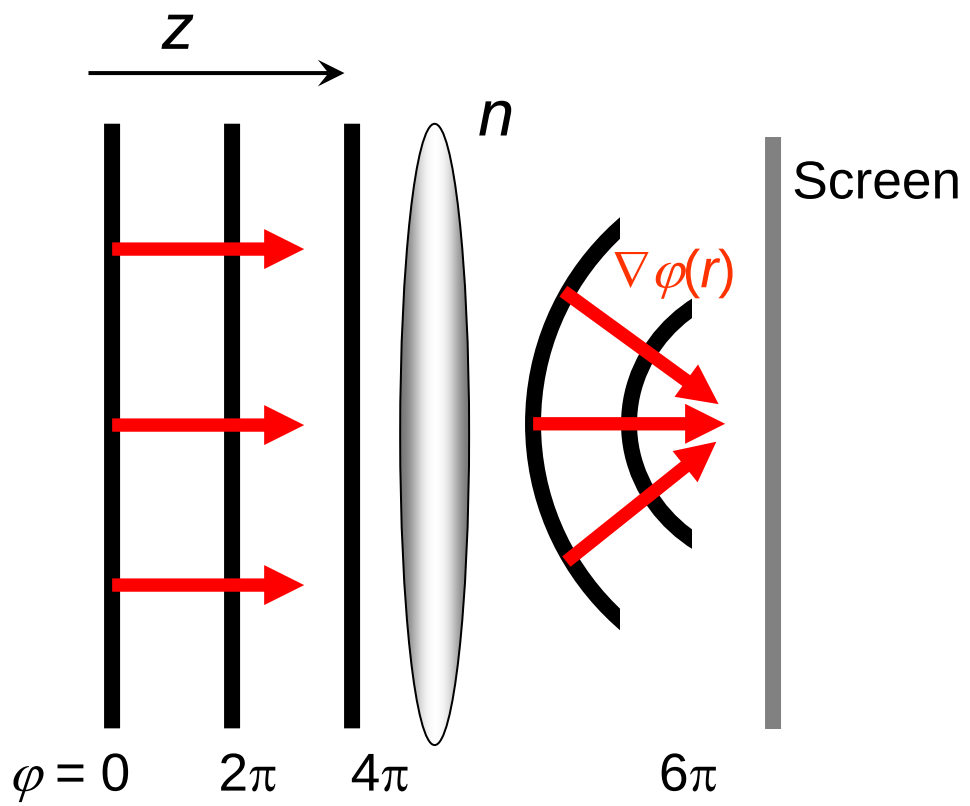

Refractive index:

phase absorption

$n(x, y, z, \lambda) = 1 - \delta(x, y, z, \lambda) - i\beta(x, y, z, \lambda)$

Phase and dark-field contrast

Angular deviation of the normal to the wave front

Normal to the wavefront:

$$\mathbf{s}(x,y,z) \approx \left(-\frac{\partial \varphi}{\partial x}, -\frac{\partial \varphi}{\partial y}, k \right)$$

Angular deviation of the normal:

$$\Delta\alpha \approx \frac{1}{k} \left| \nabla_{\perp} \varphi(x,y,z) \right|$$

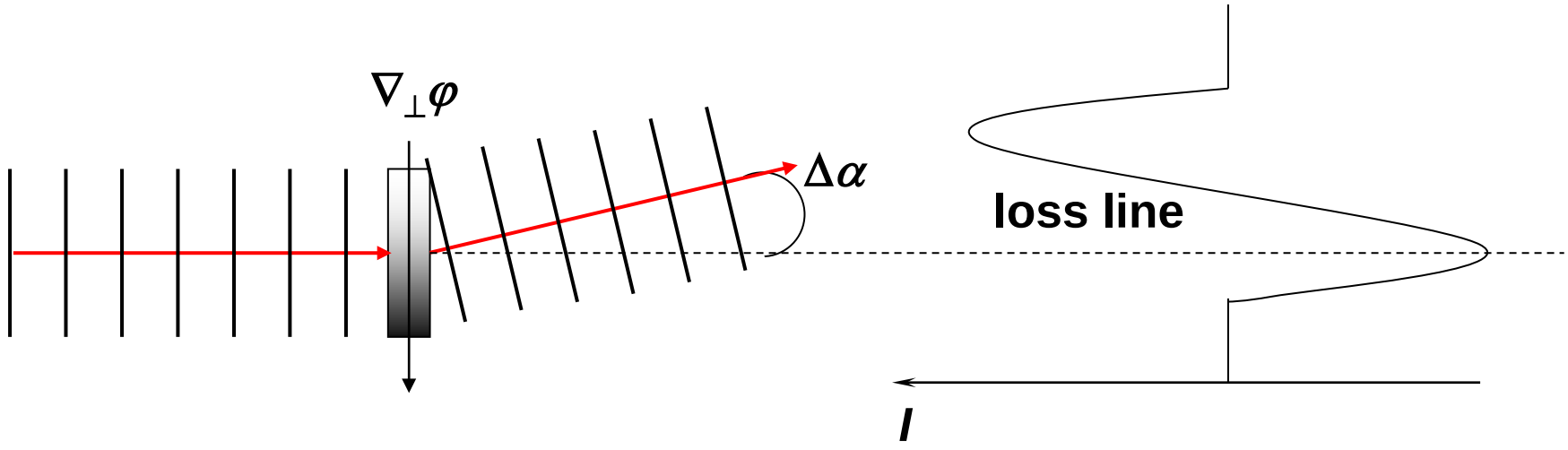

Phase and dark-field contrast

Phase-contrast radiography with thermal neutrons

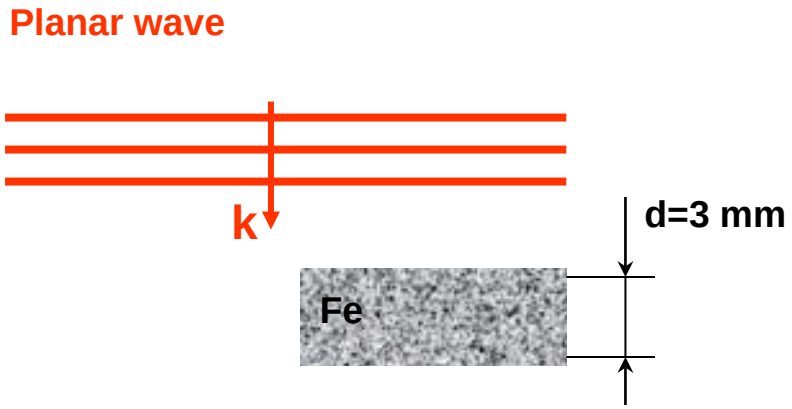

$$\delta_{Fe} = \frac{2\pi}{k^2} a_{Fe}^{coh} \rho_{Fe}$$

$$\varphi = -k \int_{-\infty}^{z} \delta(z')dz$$

$$I(x) = 1 + \frac{R\lambda}{2\pi} \varphi''(x)$$

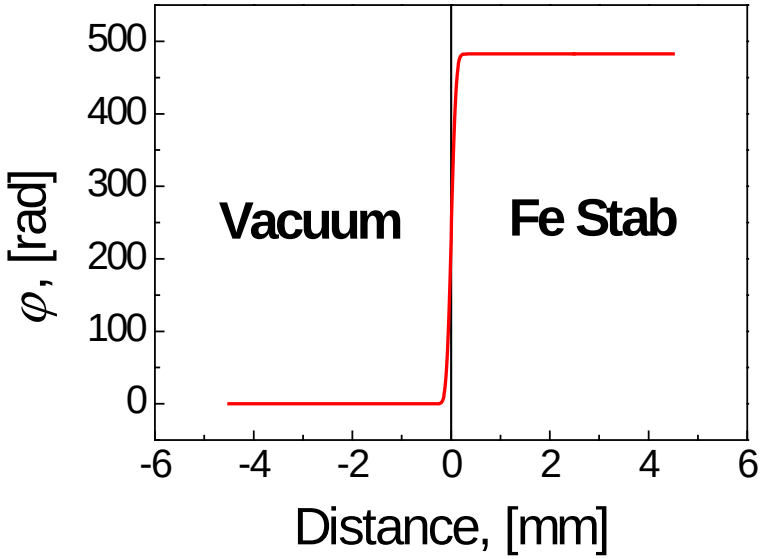

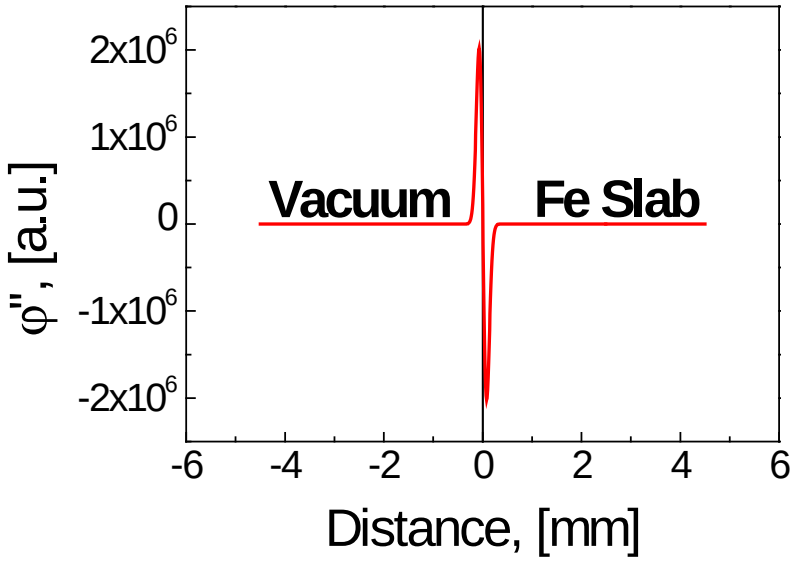

Phase and dark-field contrast

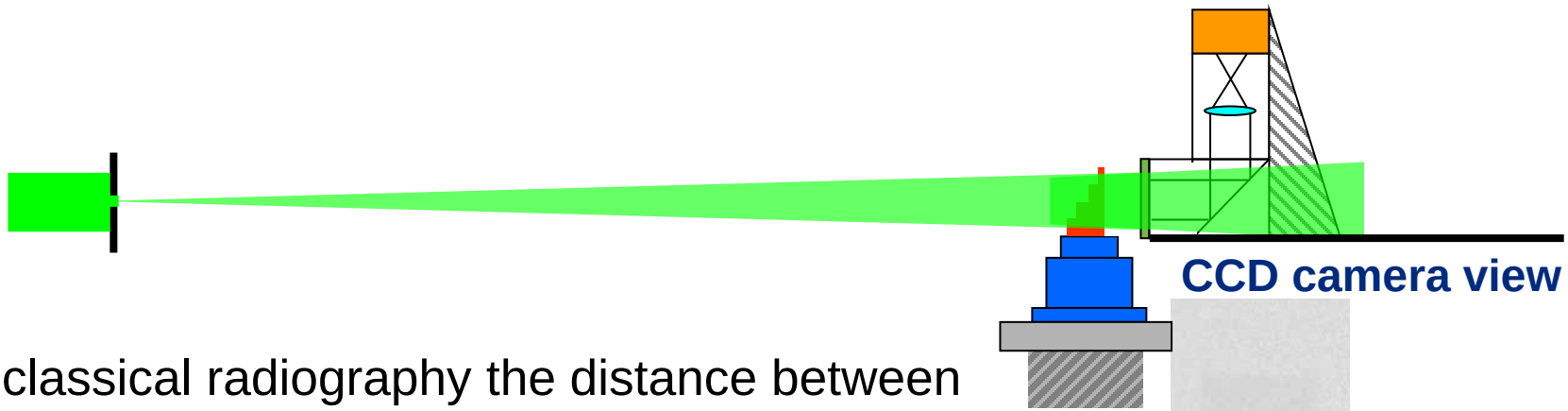

In classical radiography the distance between sample and detector is set as small as possible.

The contrast is absorption based and it is weak for low attenuating materials like aluminum.

Aluminum step wedge

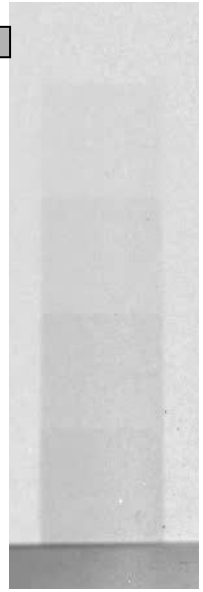

Phase and dark-field contrast

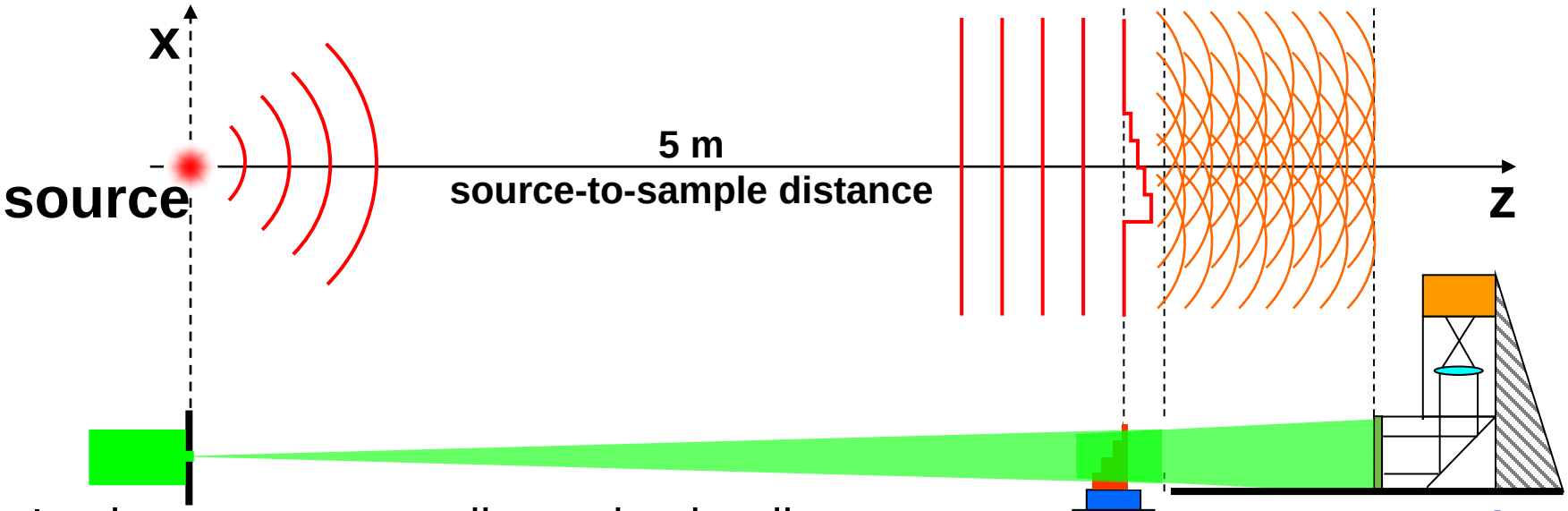

In phase-contrast radiography the distance between sample and detector is set to be large.

The small source produces spatial coherent beam. At large source-sample distance the wave front is distorted by the sample due to refraction. The obtained contrast shows edge-enhancement at large distance to detector.

CCD camera view

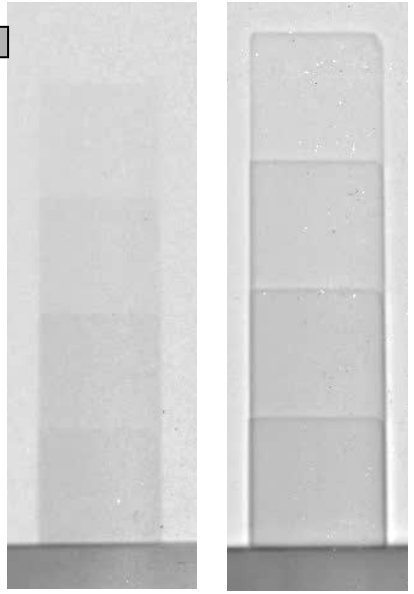

Aluminum step wedge

Phase and dark-field contrast

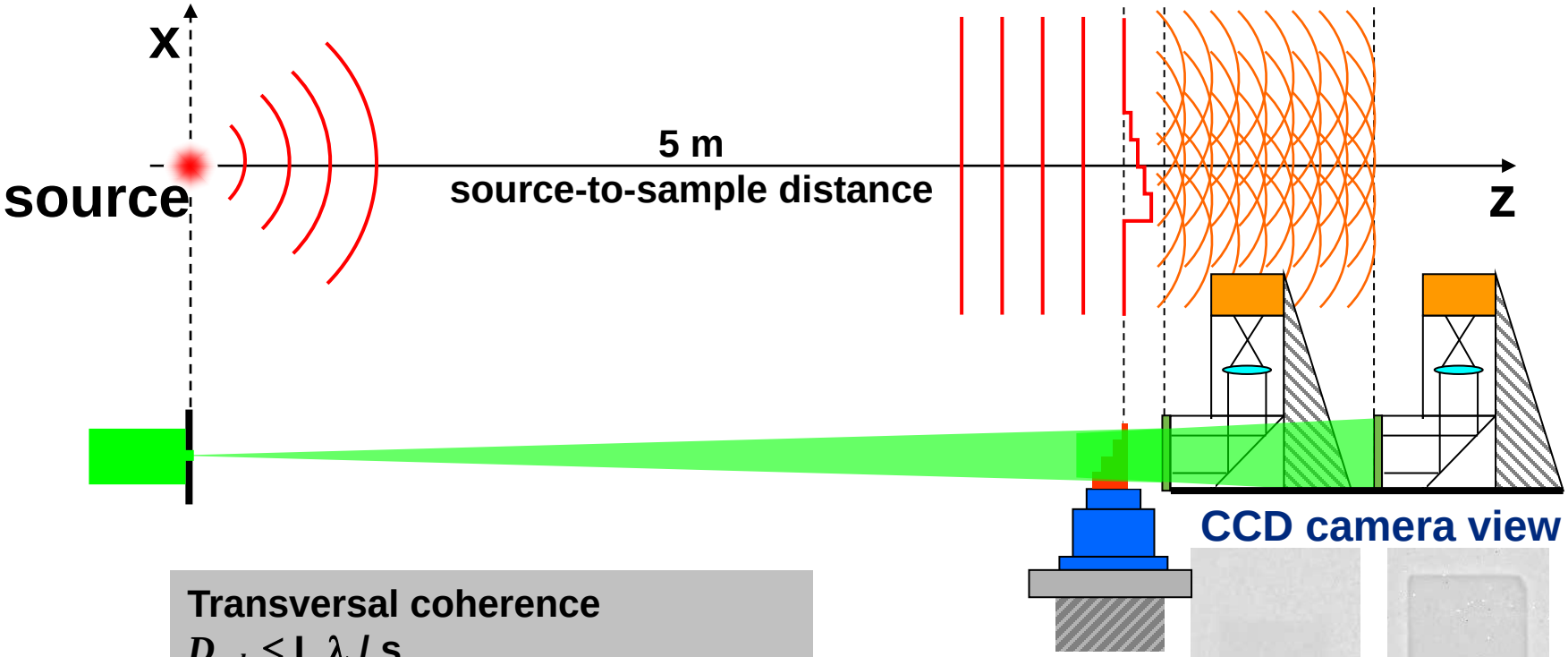

Transversal coherence

$D_{coh} \leq L \lambda / s$

Example:	**Thermal neutrons**
λ=0.2nm	**Wavelength**
L=5m	**Distance**
s=1mm	**Source size**
$\Rightarrow D_{coh} \leq$ 1µm	**Coherence length**

CCD camera view

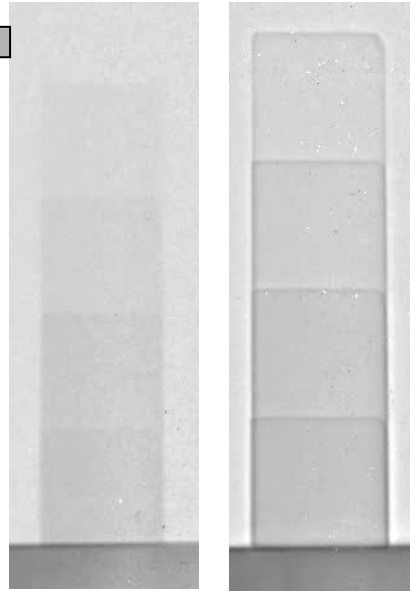

Aluminum step wedge

Phase and dark-field contrast

Pinhole 1mm, exp. time 60 min, white beam

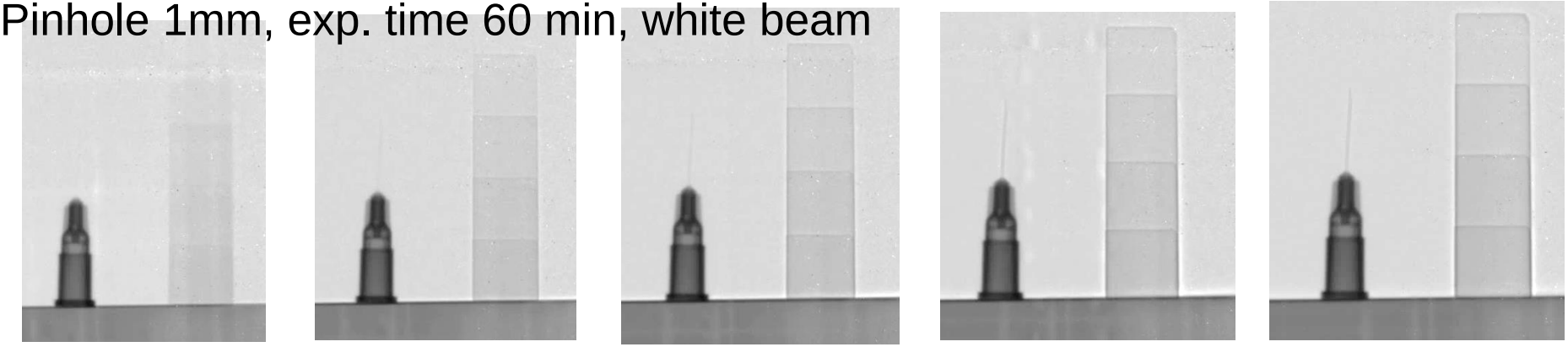

Distance, z: 0 cm to detector | 10 cm | 25 cm | 50 cm | 70 cm

Pinhole 5mm, exp. time 3 min, white beam

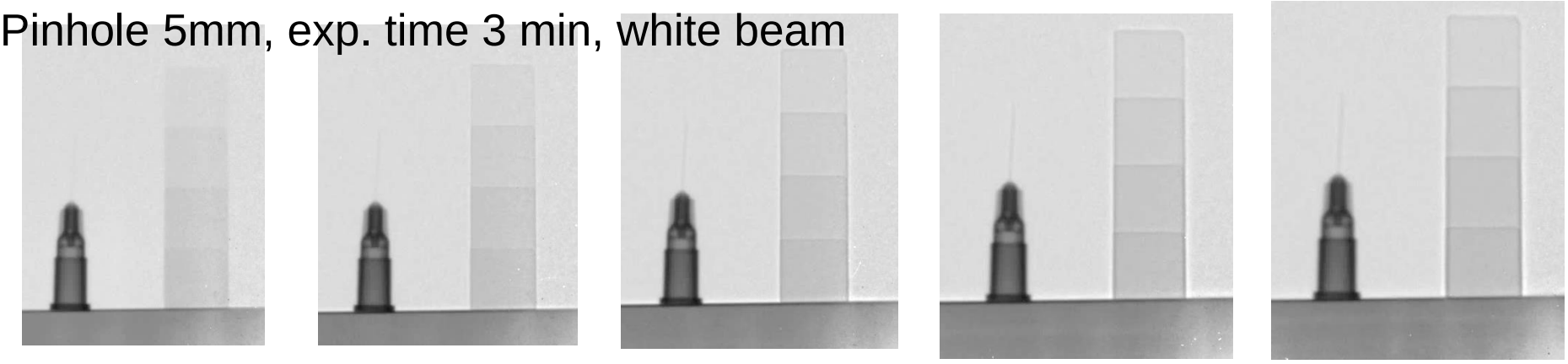

Distance, z: 0 cm to detector | 10 cm | 25 cm | 50 cm | 70 cm

Phase and dark-field contrast

Pinhole 1mm, exp. time 60 min, white beam

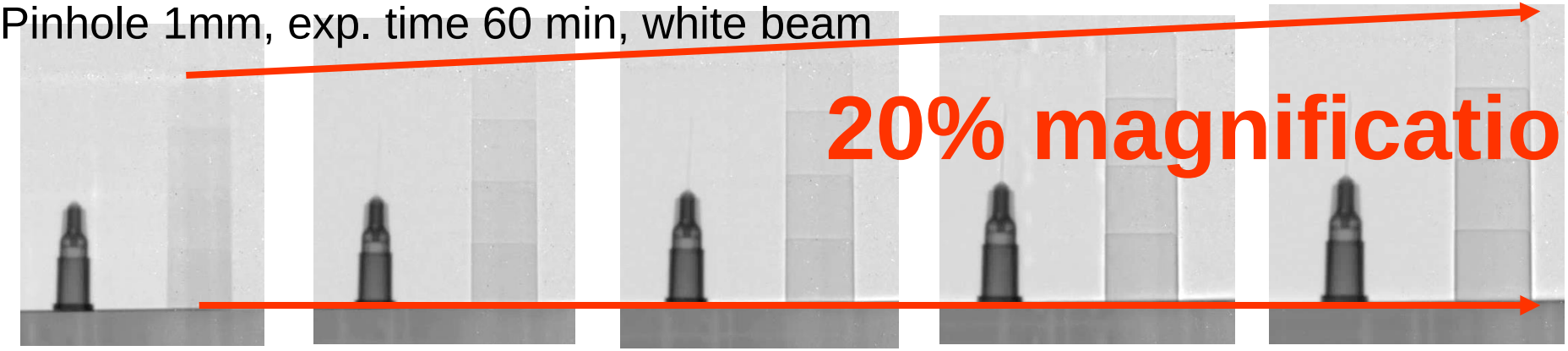

20% magnification

Distance, z: 0 cm to detector | 10 cm | 25 cm | 50 cm | 70 cm

Pinhole 5mm, exp. time 3 min, white beam

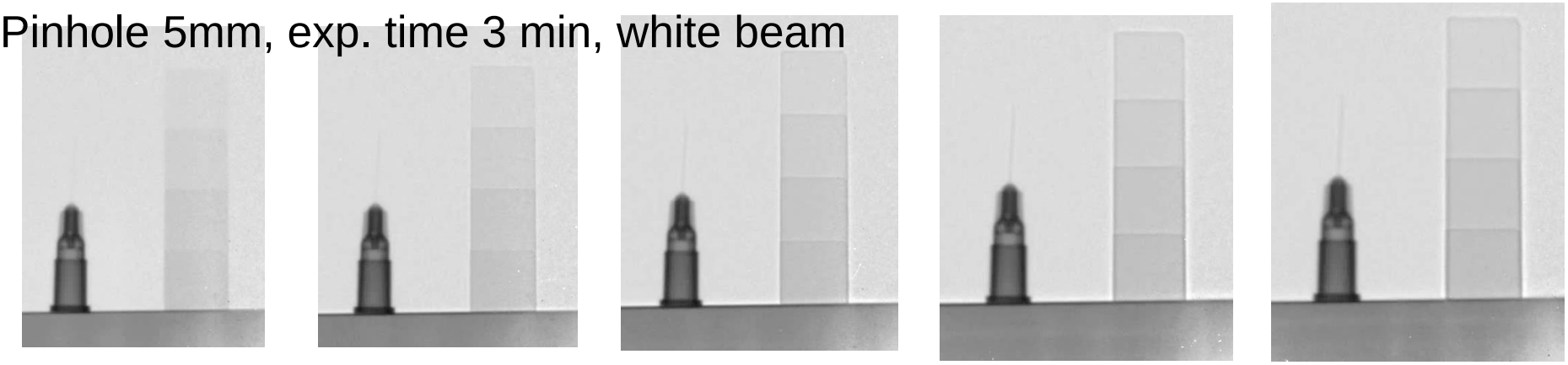

Distance, z: 0 cm to detector | 10 cm | 25 cm | 50 cm | 70 cm

The phase-contrast effect is seen at large distances z as intensity variation at the edges – edge enhancement.

Phase and dark-field contrast

The phase-contrast effect is seen at large distances between sample and detector as intensity variation at the edges – edge enhancement.

Smaller pinhole provides better resolution

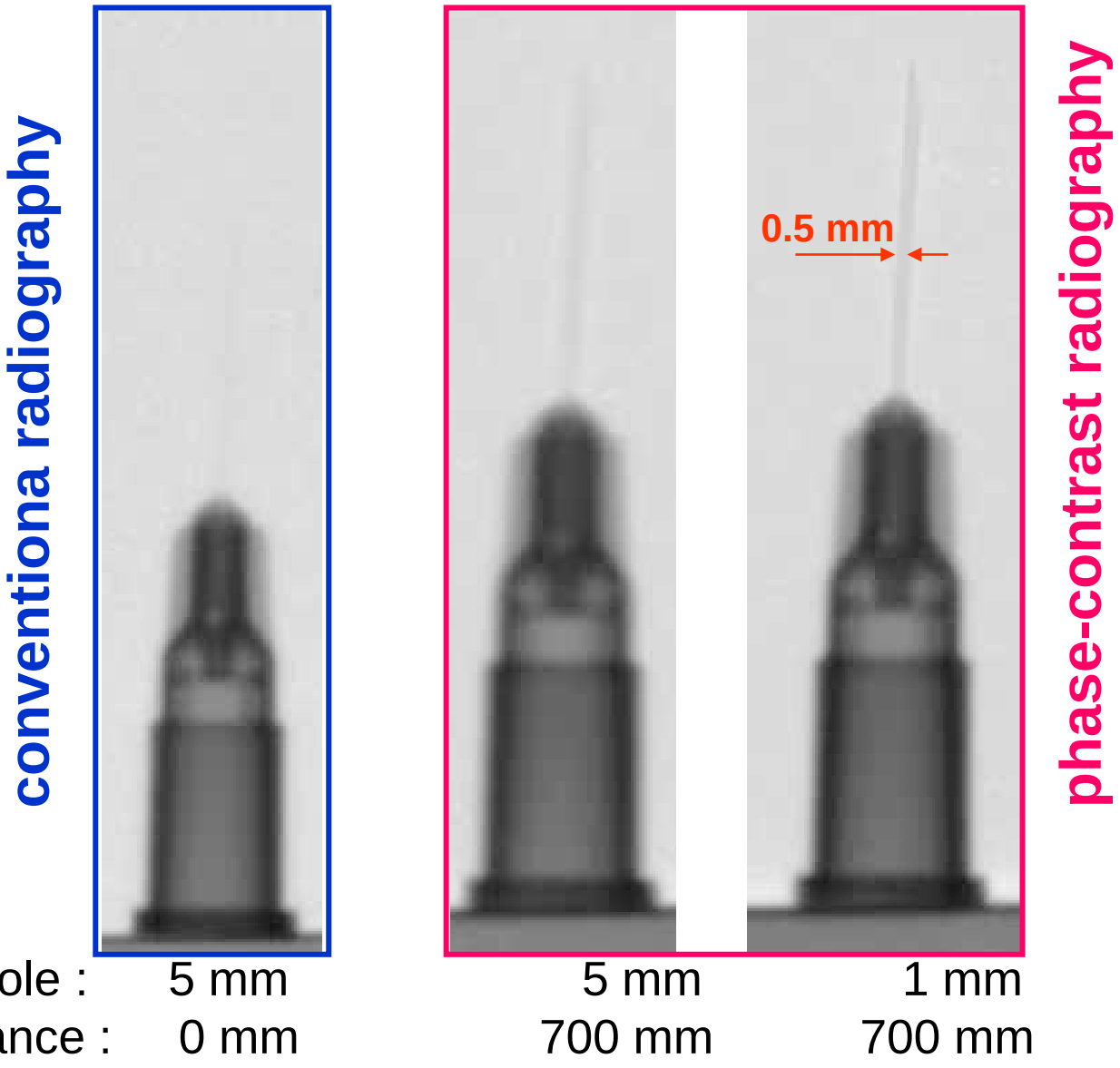

Phase and dark-field contrast

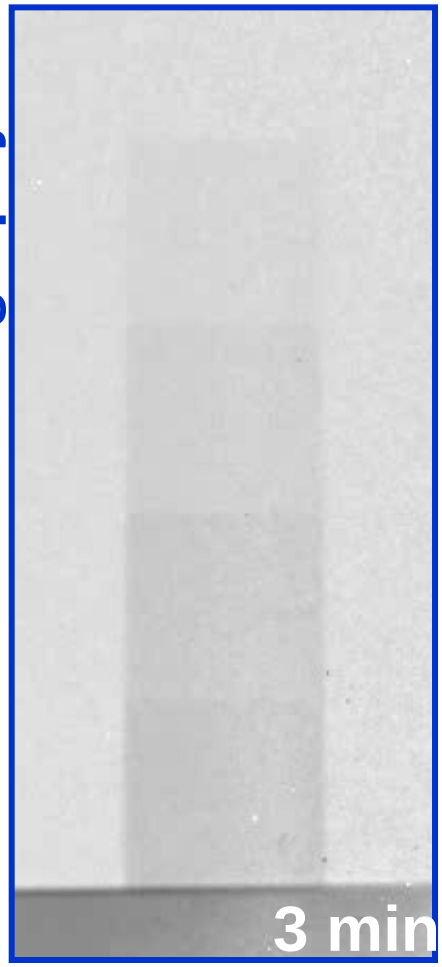

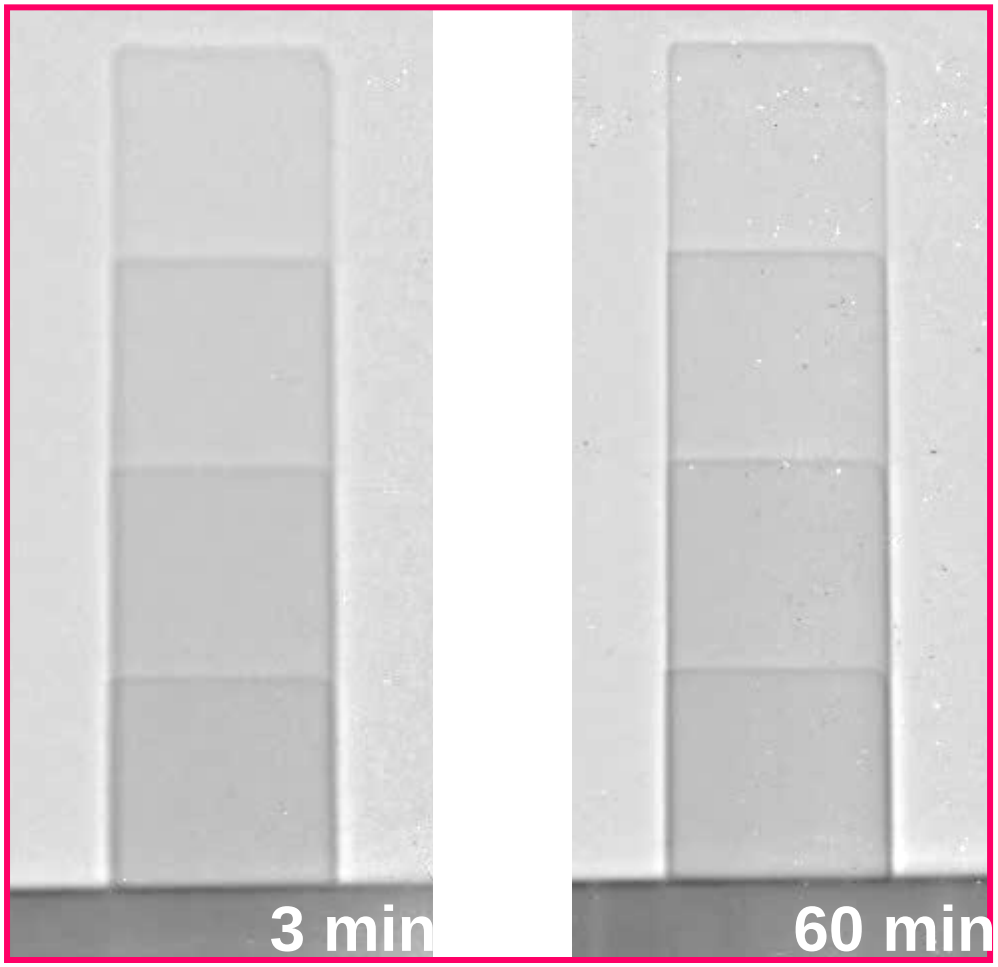

pinhole :	5 mm	5 mm	1 mm
distance :	0 mm	700 mm	700 mm

Polychromatic Phase Contrast

Pinhole: 1cm; Distance pinhole-detector: 5 m

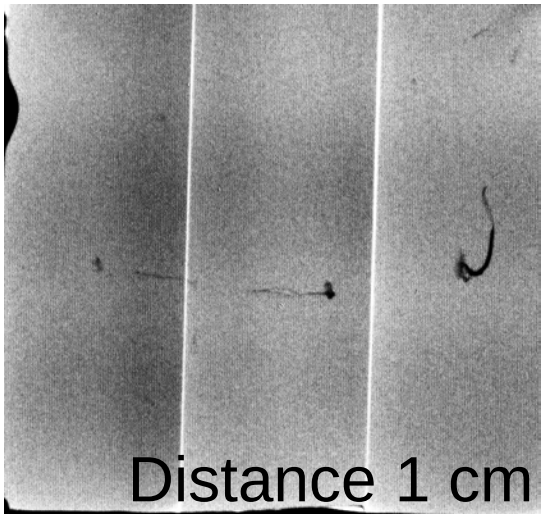

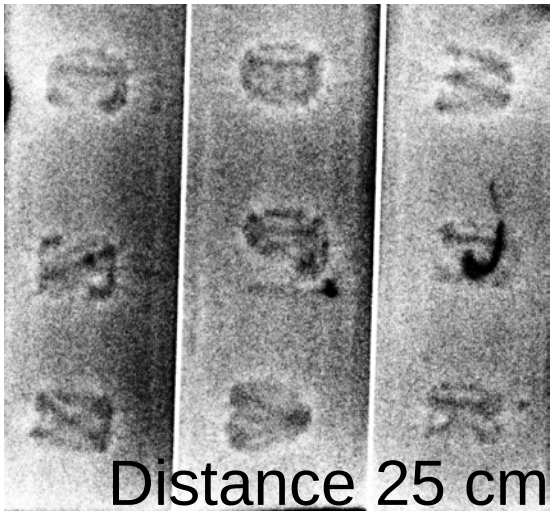

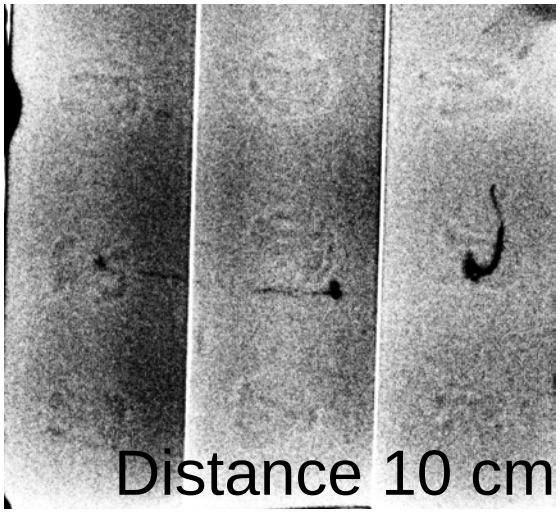

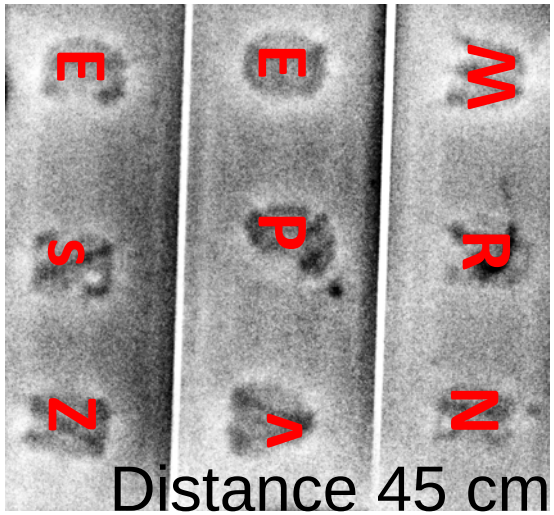

Measurement performed by F. Salvemini, ANSTO, Australia

Application: Hidden marks

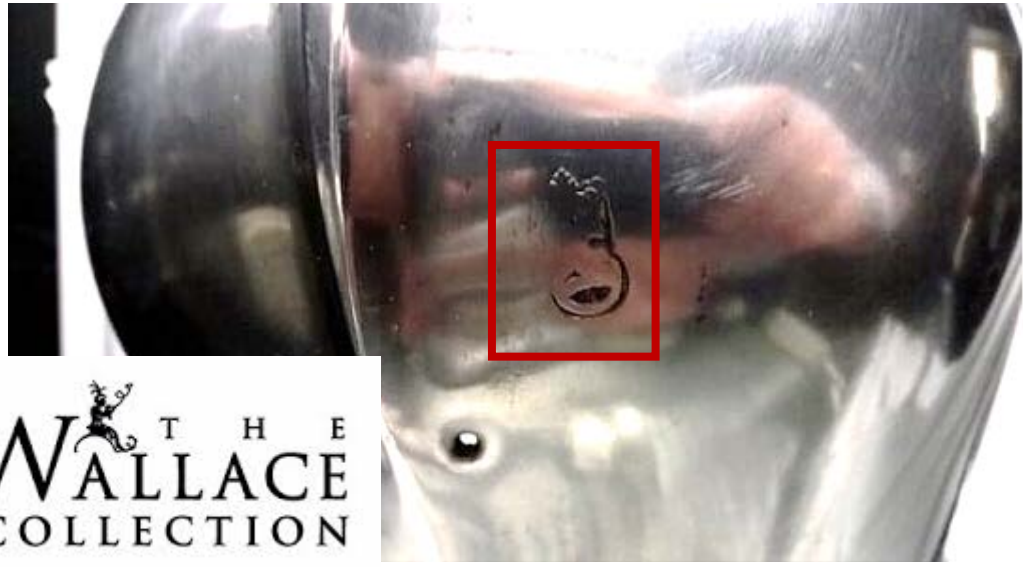

THE WALLACE COLLECTION

Williams, Alan, et al. *Studies in Conservation* 64.1 (2019): 10-15.

Application: Hidden marks

A fifteenth century Flemish open-faced helmet (sallet)

Mark belongs to the Martin Rondel of Brussels

Application: Hidden marks

The right gauntlet with a visible mark

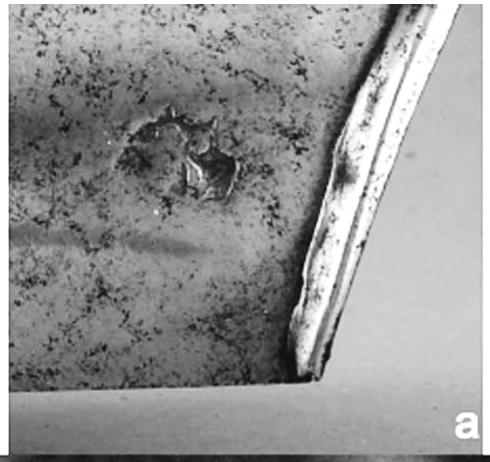

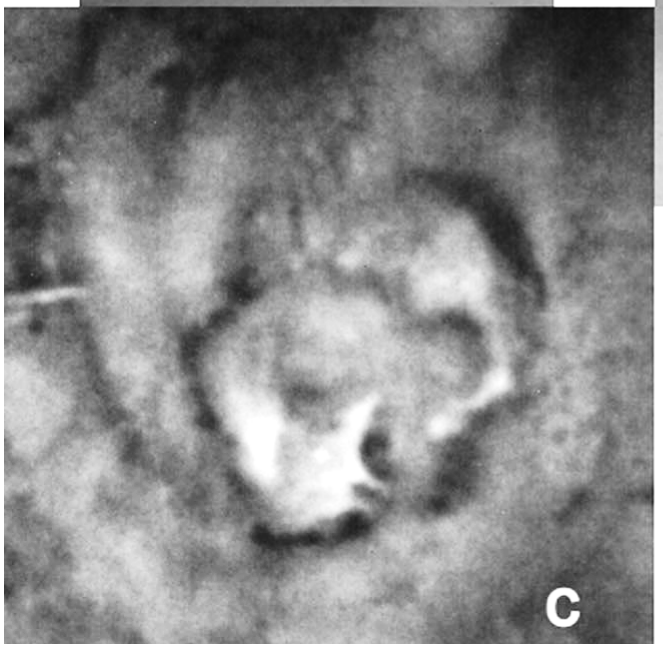

The left gauntlet with an erased mark

A threelobed leaf which is attributed to the armourer Konrad Treytz of Innsbruck

Williams, Alan, et al. *Studies in Conservation* 64.1 (2019): 10-15.

Application: Hidden marks

Breastplate c.1600 originally from the arsenal at Solothurn

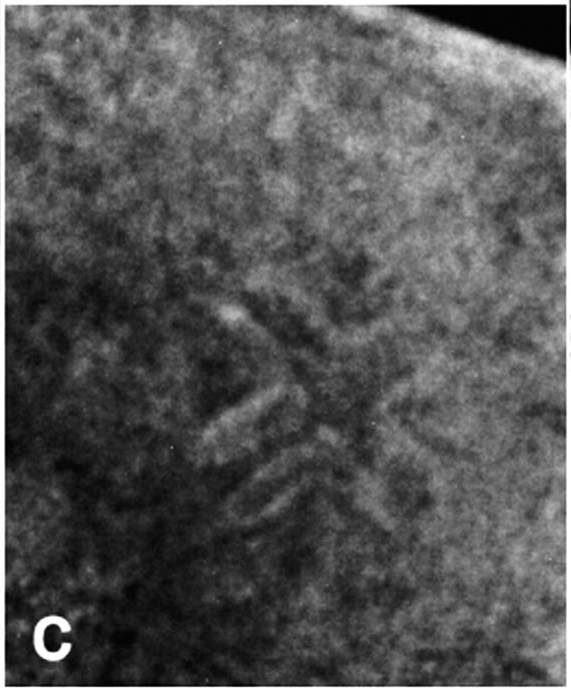

St. Andrew's cross

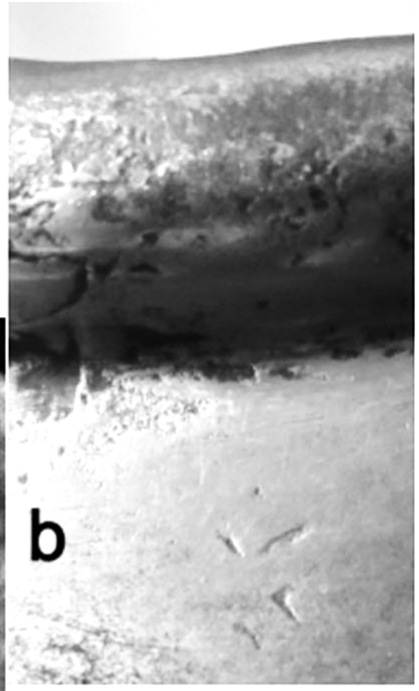

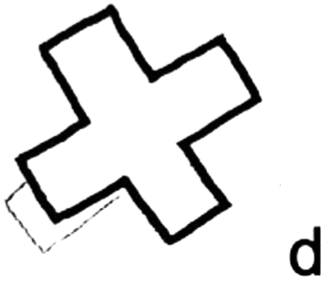

Williams, Alan, et al. *Studies in Conservation* 64.1 (2019): 10-15.

Phase and dark-field contrast

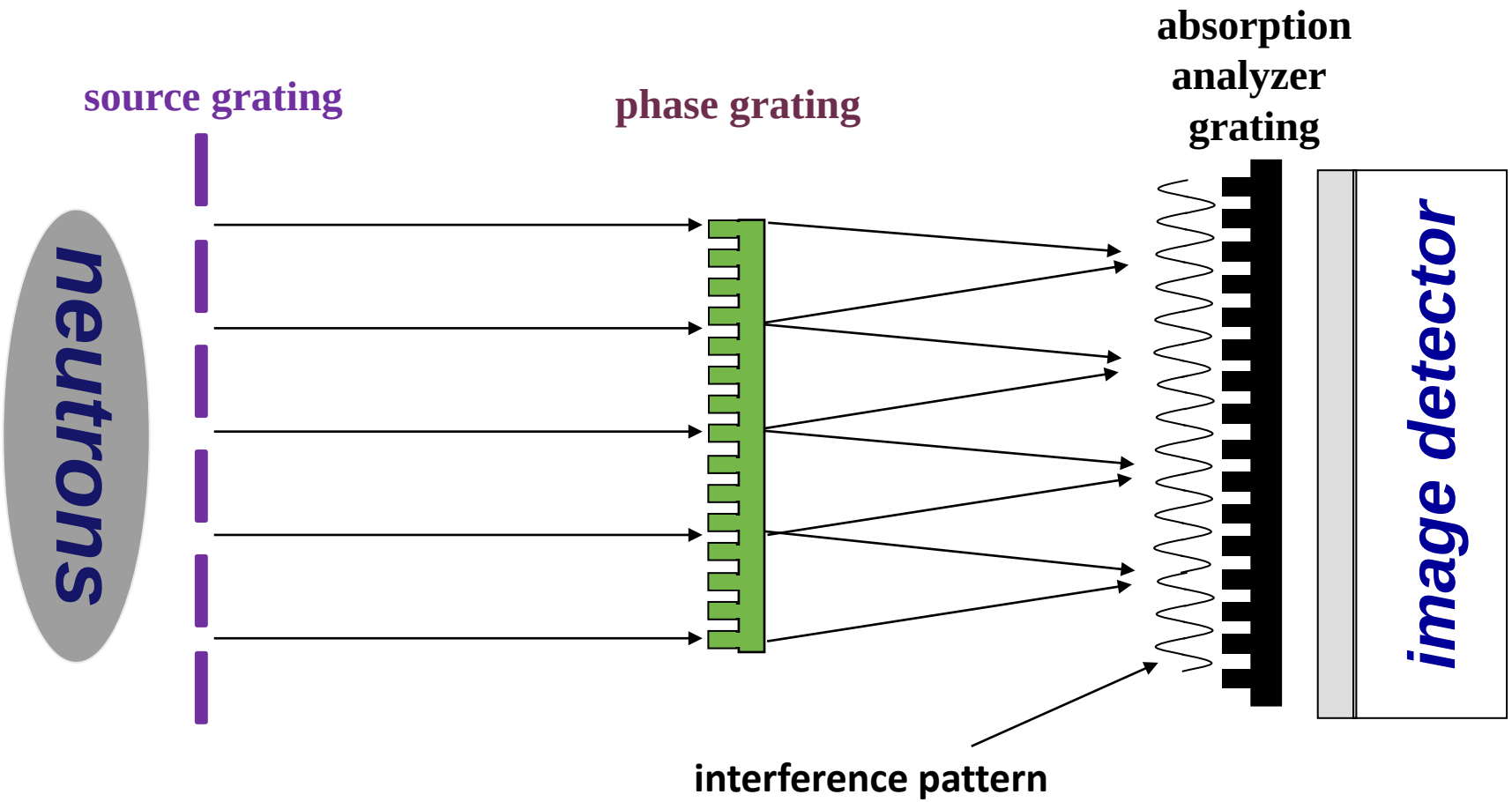

A source grating with stripes of a few hundred μm width produces an array of multiple line sources that define a spatially coherent beam illuminating a phase grating.

Phase and dark-field contrast

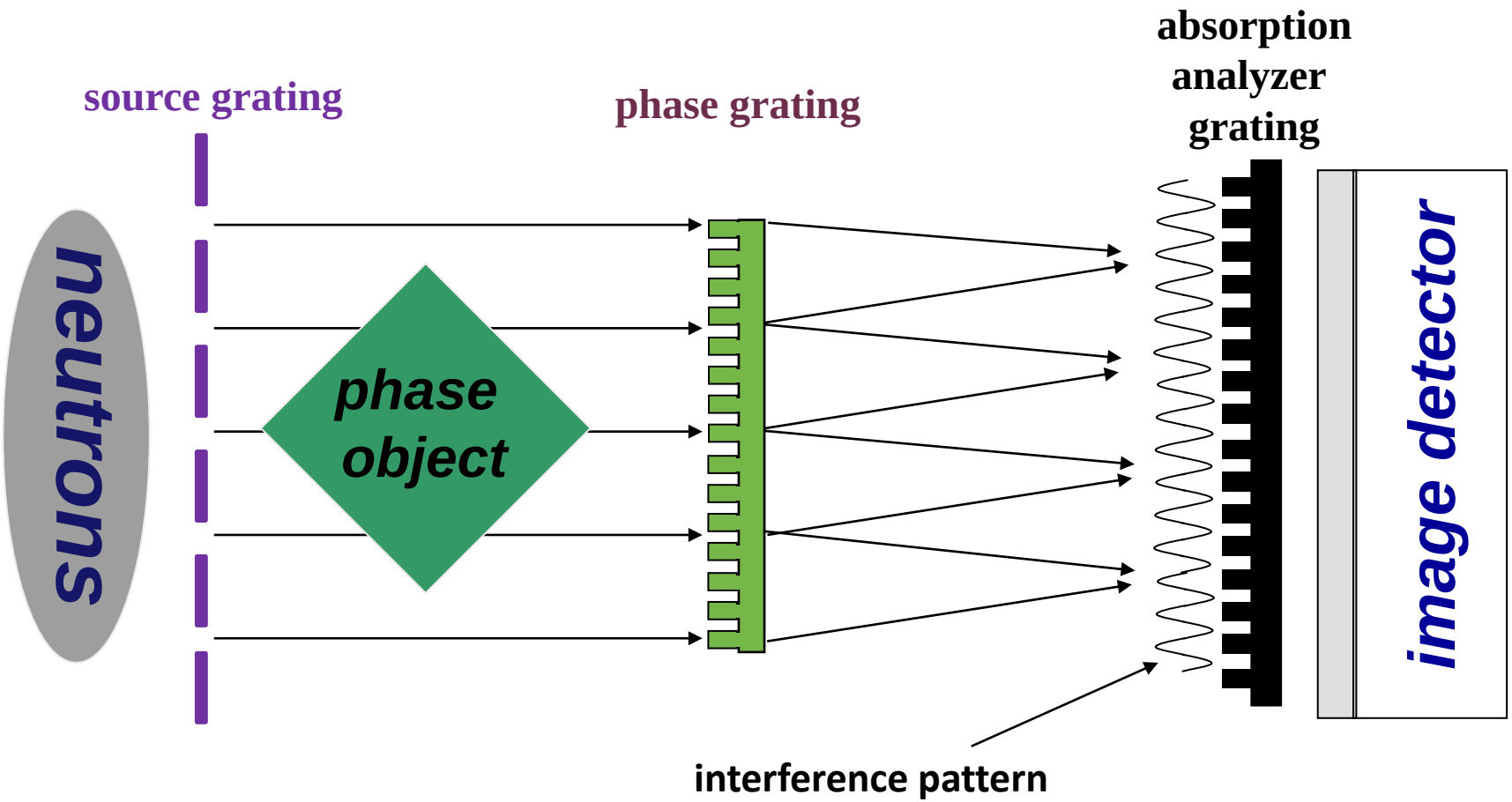

At a certain distance behind the phase grating, an interferential pattern can be observed. The structure of this pattern, which is beyond the spatial resolution of the imaging detectors, can be resolved by scanning an analyser grating through the beam in a transverse direction.

Grating interferometer

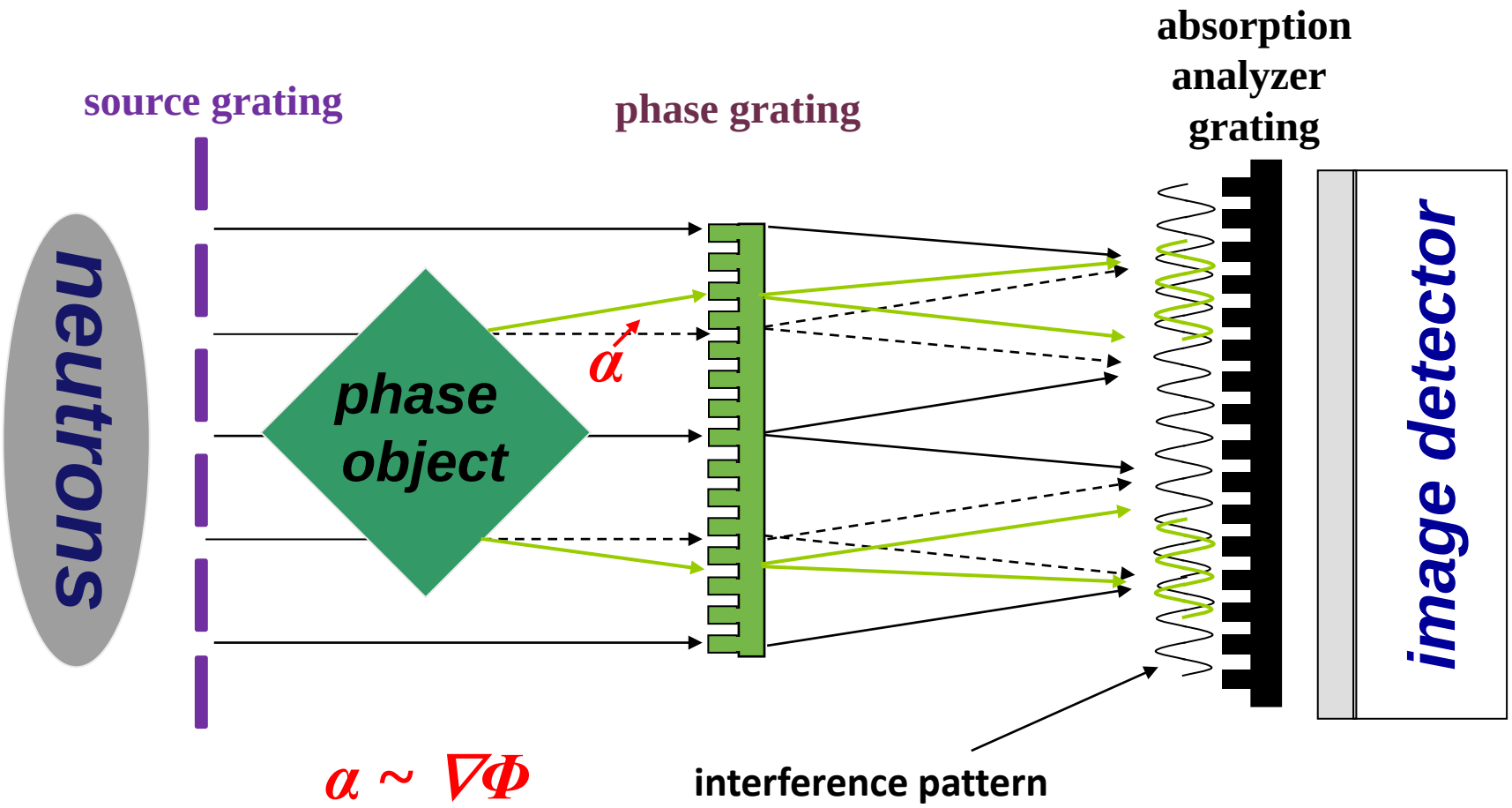

The presence of a sample distorts the interference pattern locally. Detection and analysis of the pattern yields information about phase effects, small angle scattering and attenuation introduced by the sample.

Phase and dark-field contrast

When magnetic samples are investigated by grating interferometry, neutrons are scattered by the volume between two domains and in return cause a reduced amplitude of the interferential pattern. This change in the amplitude can be detected for each pixel and a corresponding amplitude map can be obtained. In this way the domain walls can be visualized.

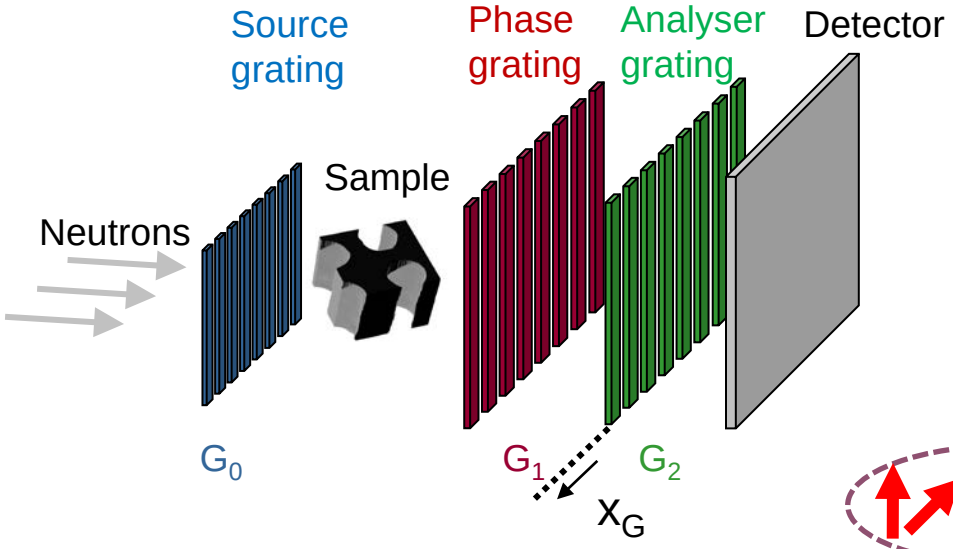

Multiple refractions at the domain walls results in local degradation of the beam coherence (decrease of the amplitude in the interference pattern).

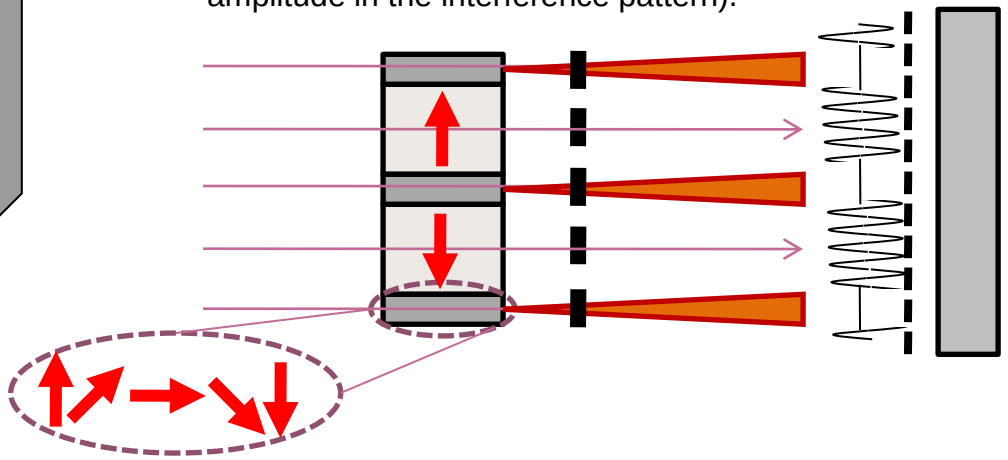

Phase and dark-field contrast

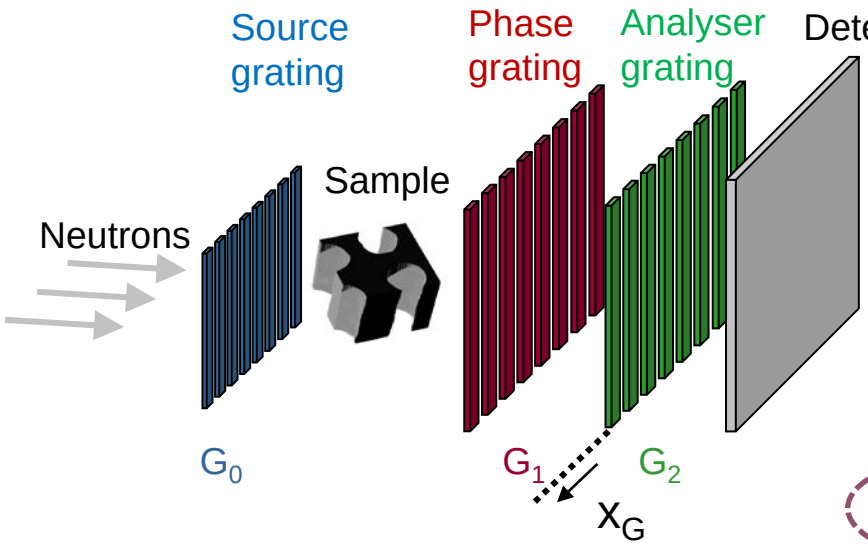

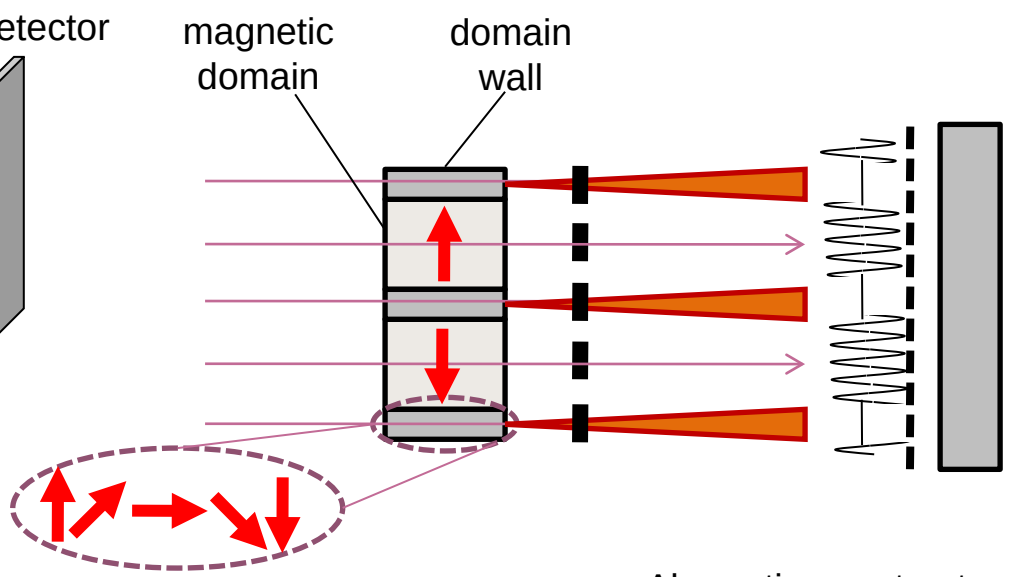

Magnetic domains in FeSi single crystal

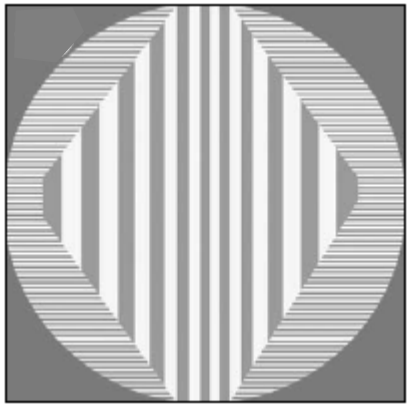

Absorption contrast (conventional radiography)

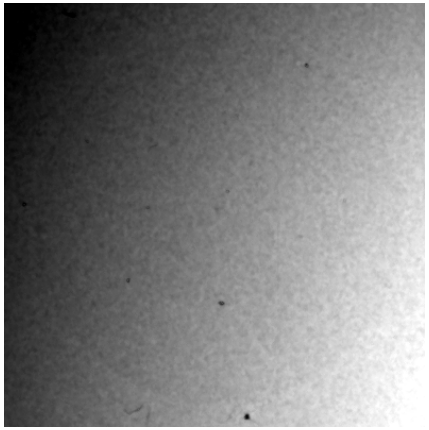

Ch. Grünzweig, et al. *Applied Physics Letters* 93.11 (2008): 112504.

Phase and dark-field contrast

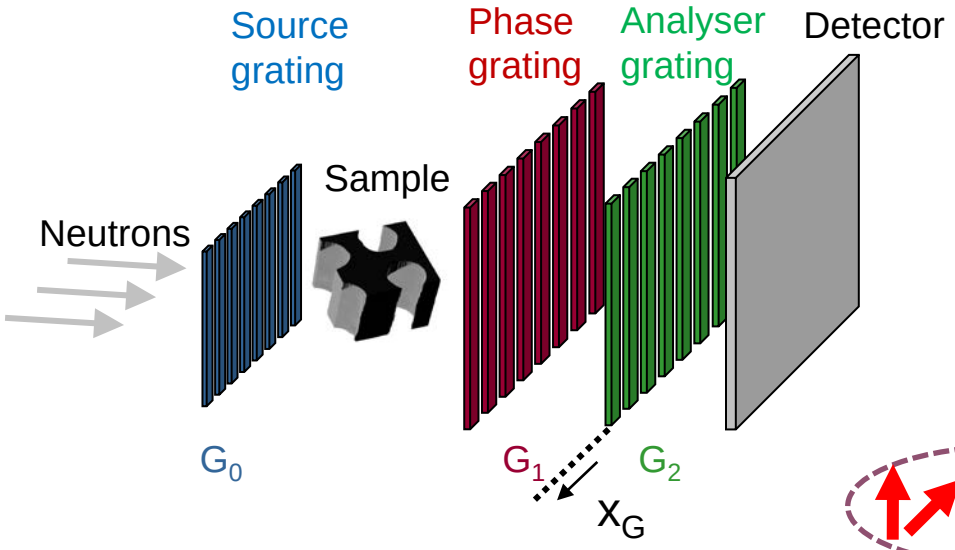

Multiple refractions at the domain walls results in local degradation of the beam coherence (decrease of the amplitude in the interference pattern).

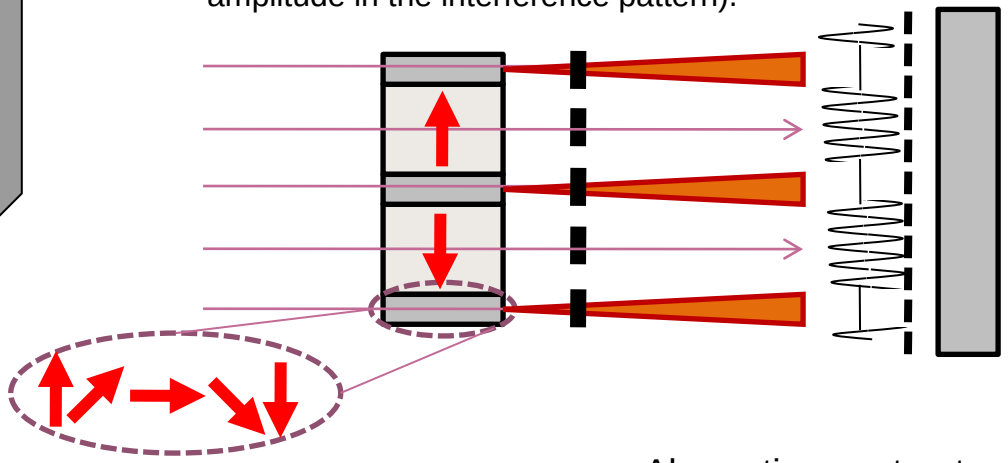

Magnetic domains in FeSi single crystal

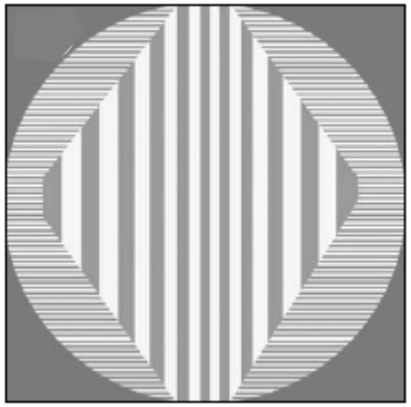

Magnetic domain structure in the sample is obtained by analyzing the amplitude of the oscillation.

Dark-field contrast

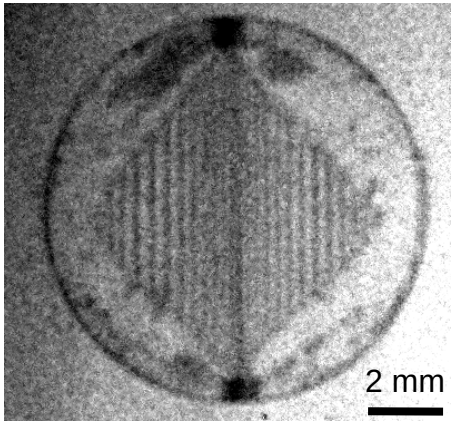

Absorption contrast (conventional radiography)

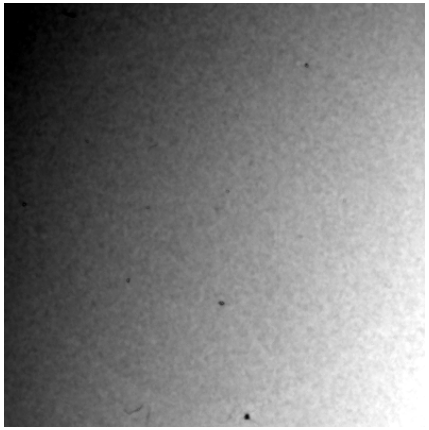

Ch. Grünzweig, et al. *Applied Physics Letters* 93.11 (2008): 112504.

Phase and dark-field contrast

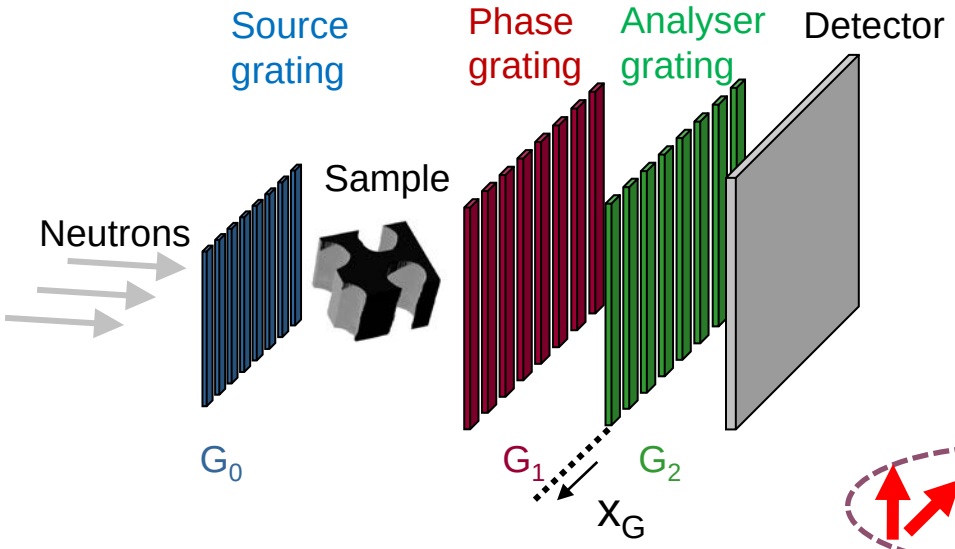

Multiple refractions at the domain walls results in local degradation of the beam coherence (decrease of the amplitude in the interference pattern).

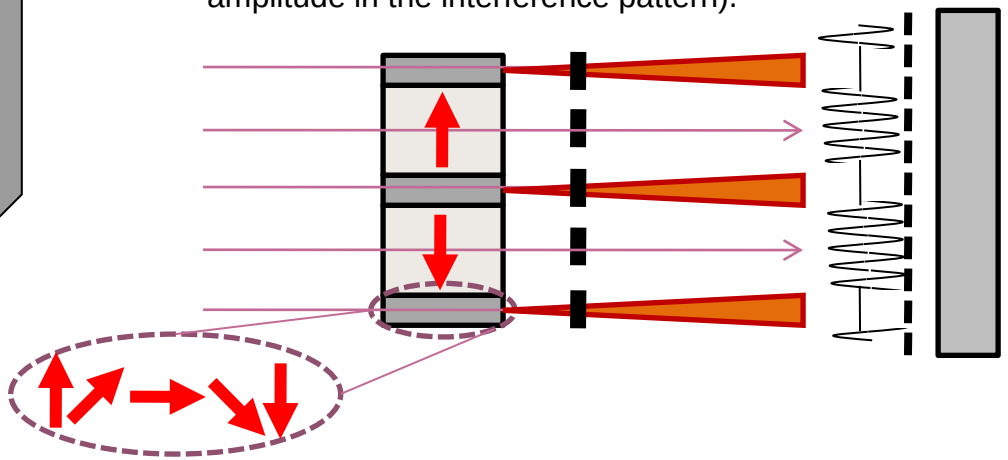

Magnetic domains in a bulky FeSi single crystal

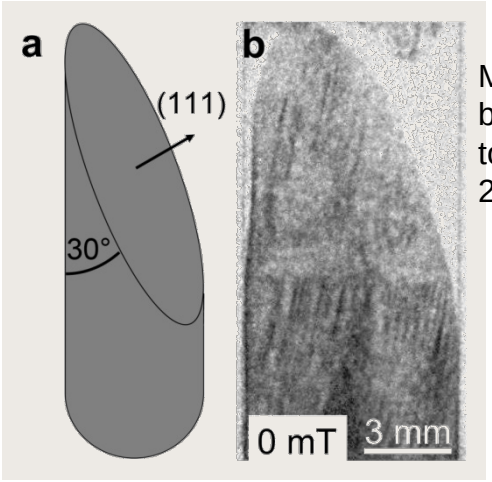

Magnetic domain structure can be visualized in 3D by applying tomographic reconstruction from 2D angular projections

3D domain distribution

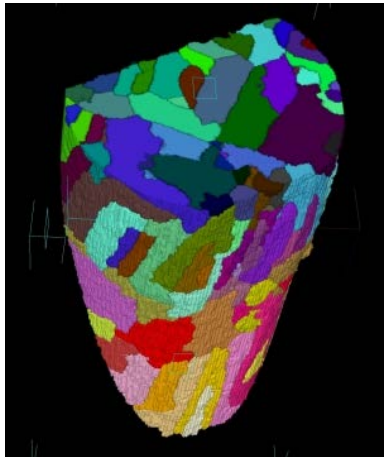

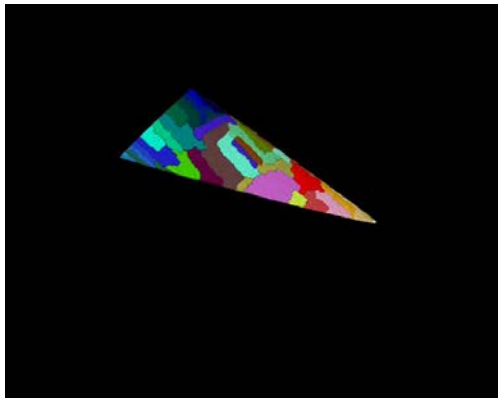

I. Manke et al, Nature Communications 1 (8), p.125 (2010)

Imaging with polarized neutrons

Radiography image of a bar magnet taken with polarized neutrons

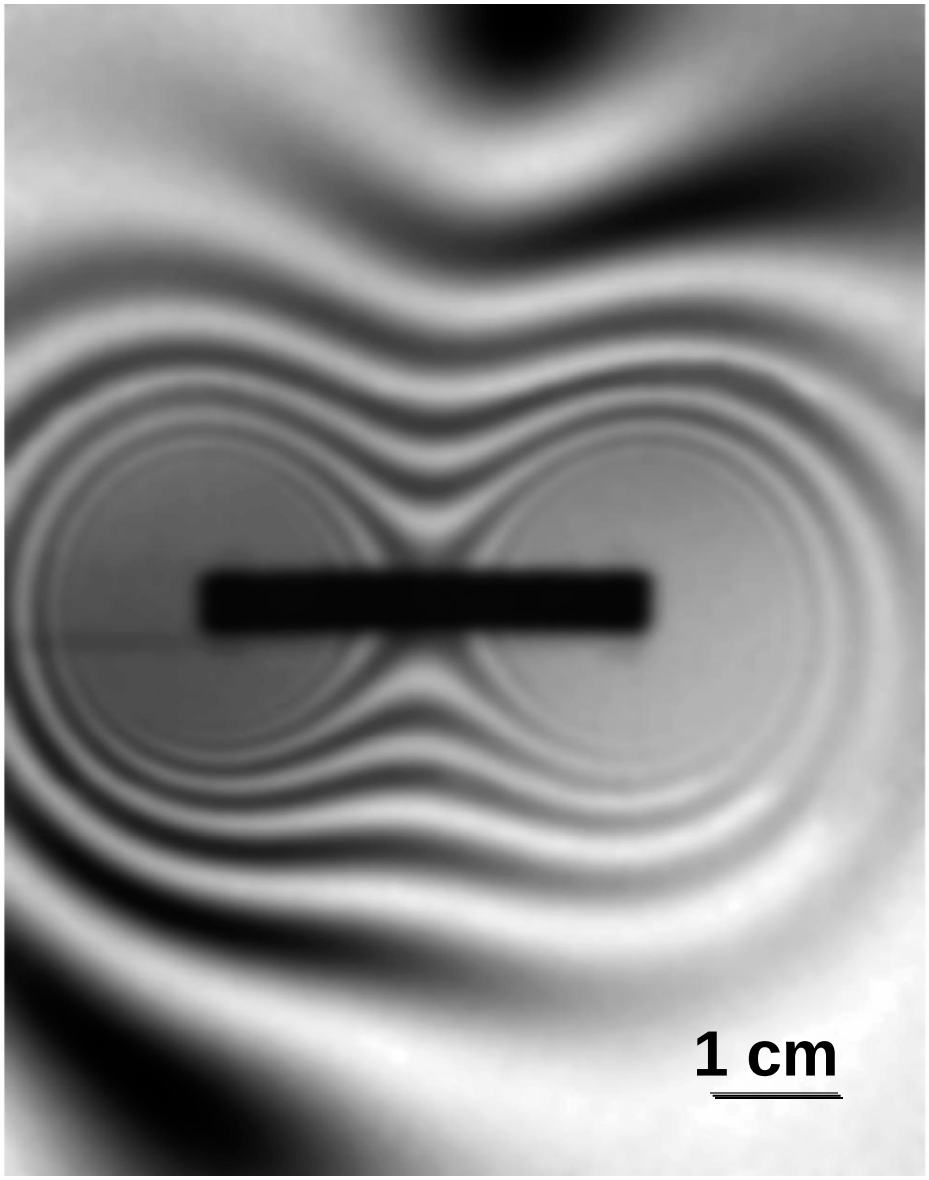

N. Kardjilov, et al,
Nature Physics 4, 399-403, (2008)

Imaging with polarized neutrons

Polarized neutrons: a collection of neutrons whose spins have a preferential orientation with respect to a particular direction in space, usually the direction of a magnetic field.

Since a neutron has a spin of 1/2, in a magnetic field H two orientations of its spin are possible: parallel or antiparallel to H.

A neutron beam is polarized if it contains a different number N of neutrons with spins oriented along (N_+) and against (N_-) the field. The degree of polarization is characterized by the quantity

$$p = (N_+ - N_-)/(N_+ + N_-)$$

Imaging with polarized neutrons

Why we use polarised neutron?

- It has a magnetic moment $\mu = -1.913\ \mu_r$
- It interacts with magnetic fields
- Its Larmor precession can be used as signal for imaging

Magnetic properties of materials can be investigated by utilising the magnetic moment of the neutron.

Imaging with polarized neutrons

Interactions of neutron spin with magnetic fields

Spin precession arround external magnetic field

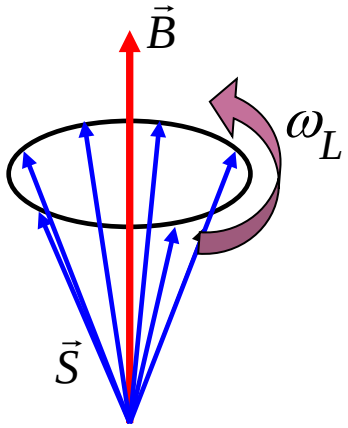

Larmor precession with a frequency:

$$\omega_L = \gamma B$$

$$\gamma = 1.83 \cdot 10^8 \frac{rad}{s \cdot T}$$ (gyromagnetic ratio)

The magnetic moment is antiparallel to the internal angular momentum of the neutron described by a spin S with the quantum number s = 1/2.

Imaging with polarized neutrons

Principle

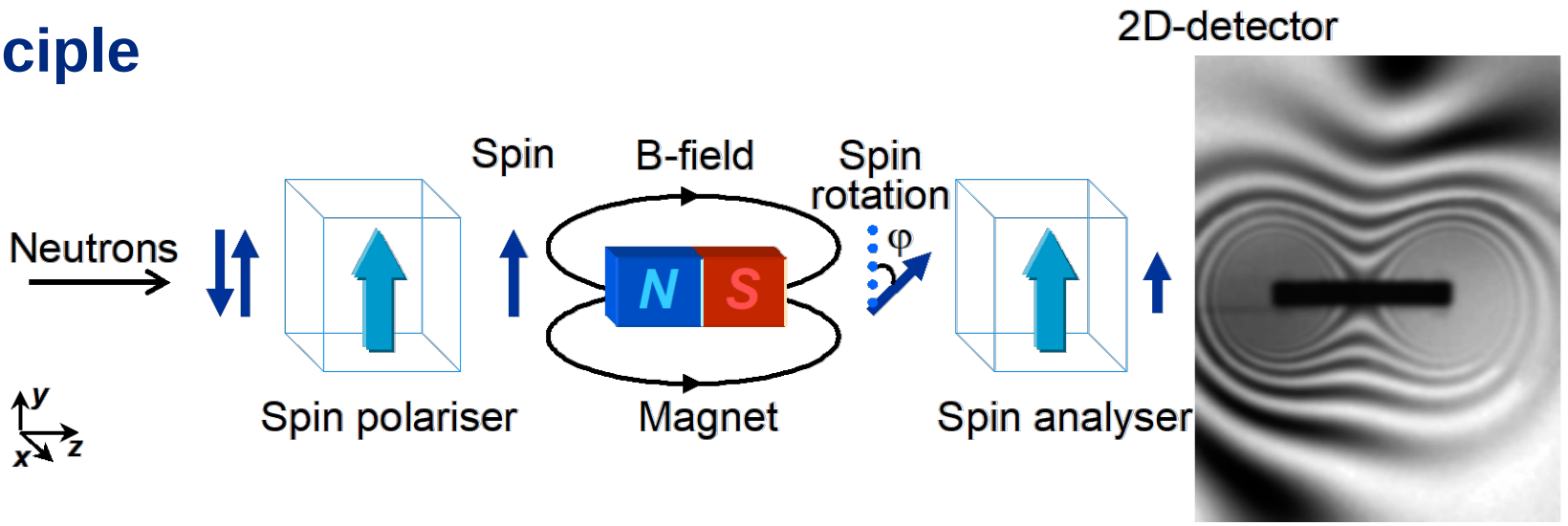

$$\varphi = \omega_L t = \frac{\gamma_L}{v} \int_{path} H ds$$

For the imaging setup, a polariser and analyser are used to select a defined neutron polarisation or orientation of the magnetic moment and to convert the precession angle φ of the neutron spin after transmission through the magnetic field or sample to imaging contrast, respectively.

N. Kardjilov, et al, Nature Physics 4, 399-403, (2008)

Imaging with polarized neutrons

Solid-state bender polarizer

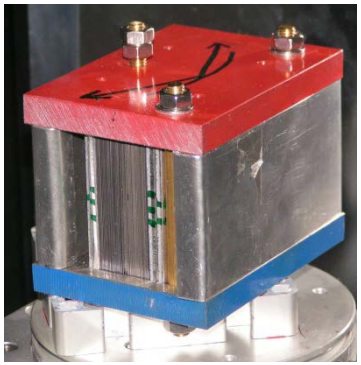

The bent supermirror plates reflect only one spin component. The other component is absorbed in a Gd layer on the back.

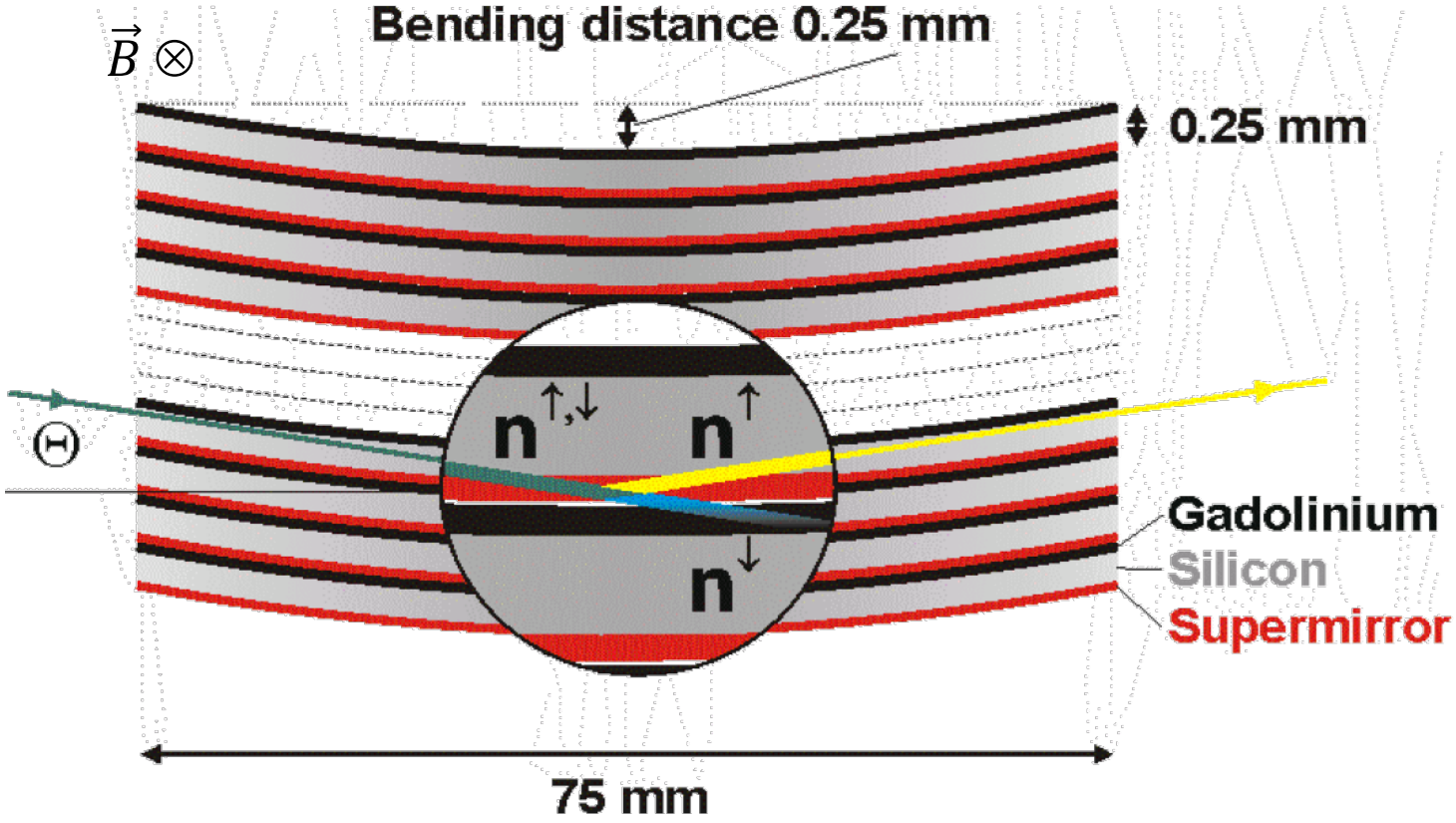

Imaging with polarized neutrons

Solid-state bender polarizer

Refractive index: $n = 1 - \lambda^2 \left(\frac{N \cdot b_c}{2\pi} \pm \frac{\mu m B}{h^2} \right)$

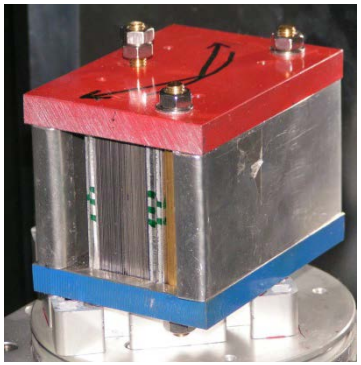

The bent supermirror plates reflect only one spin component. The other component is absorbed in a Gd layer on the back.

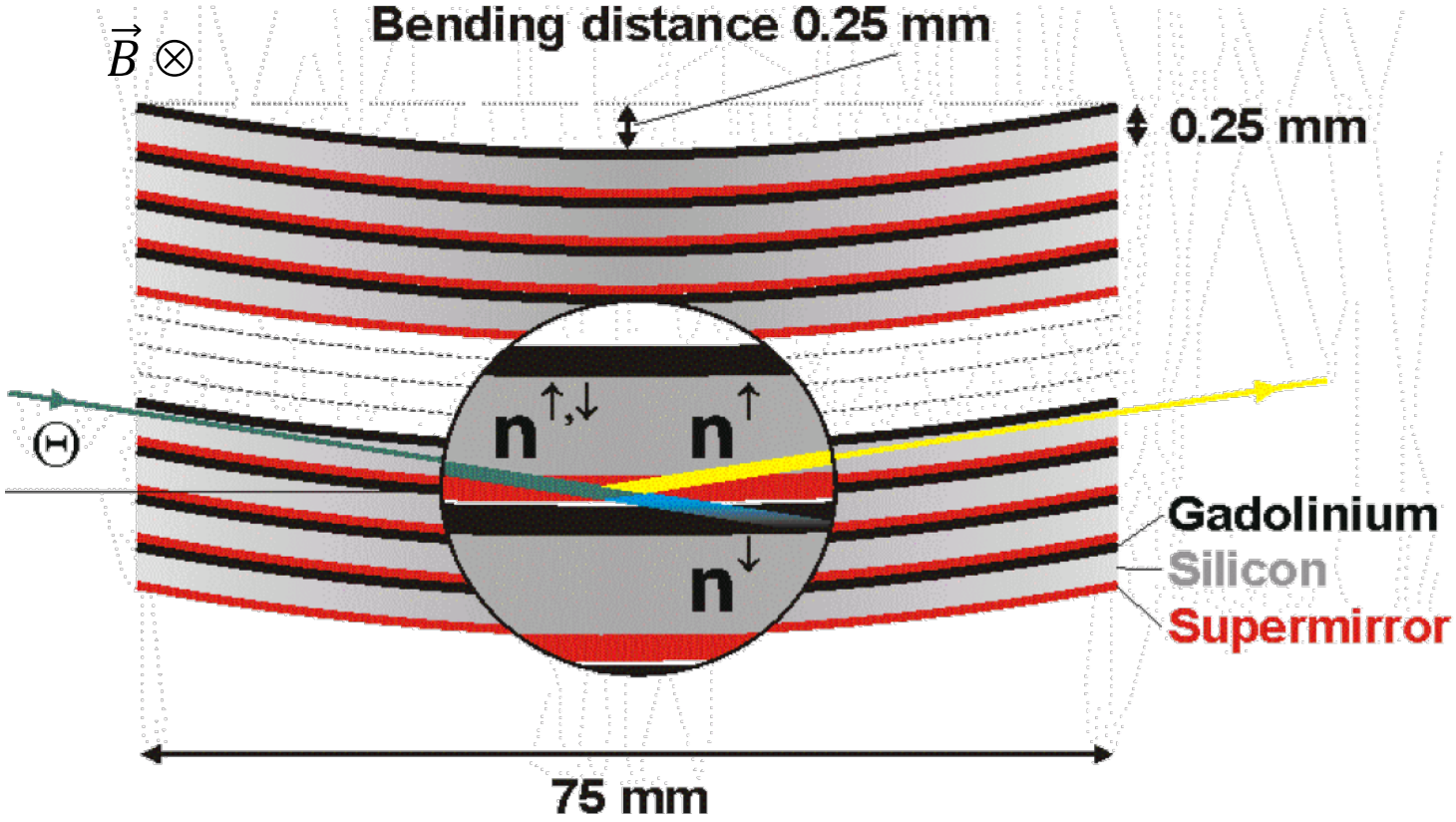

The magnetic field B provides different refractive indexes for the spin components alligned parallel and antiparallel to it.

Imaging with polarized neutrons

Example
Instrument: V7 (CONRAD) at HZB, Berlin
Monochromatic beam with wavelength of 4.2 Å
Spatial resolution: 0.2 mm/pixel

Experimental sketch:

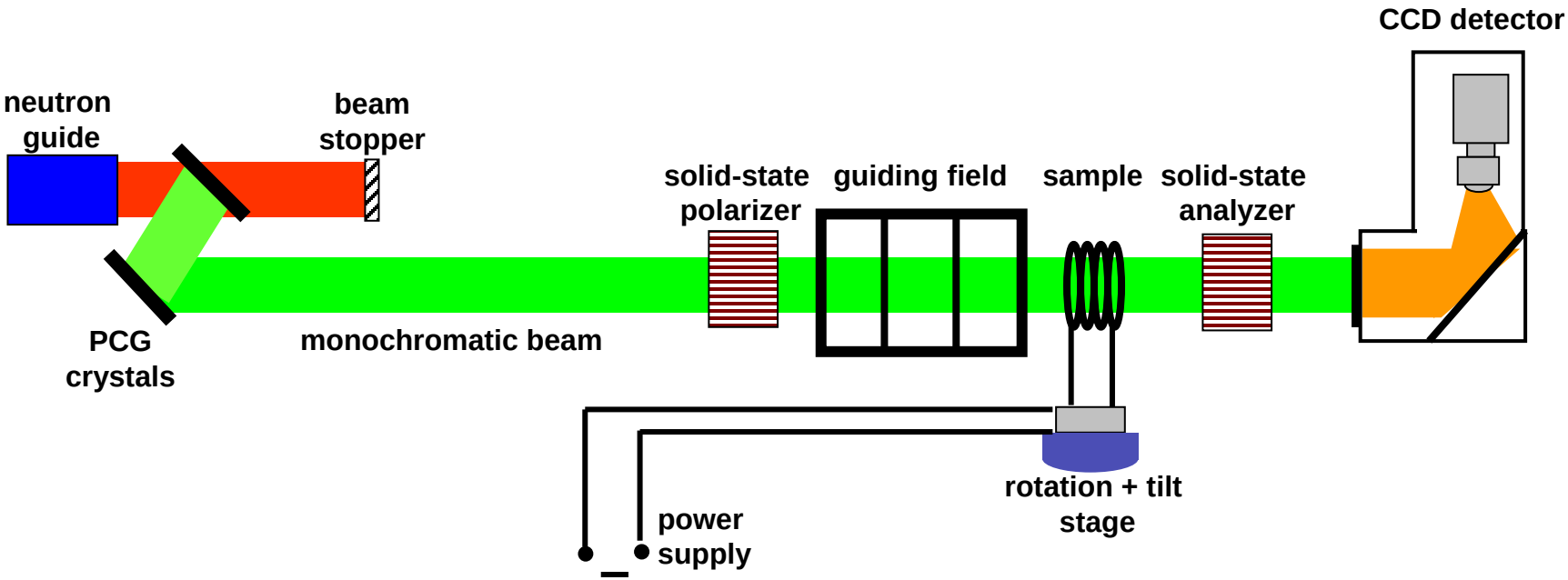

Imaging with polarized neutrons

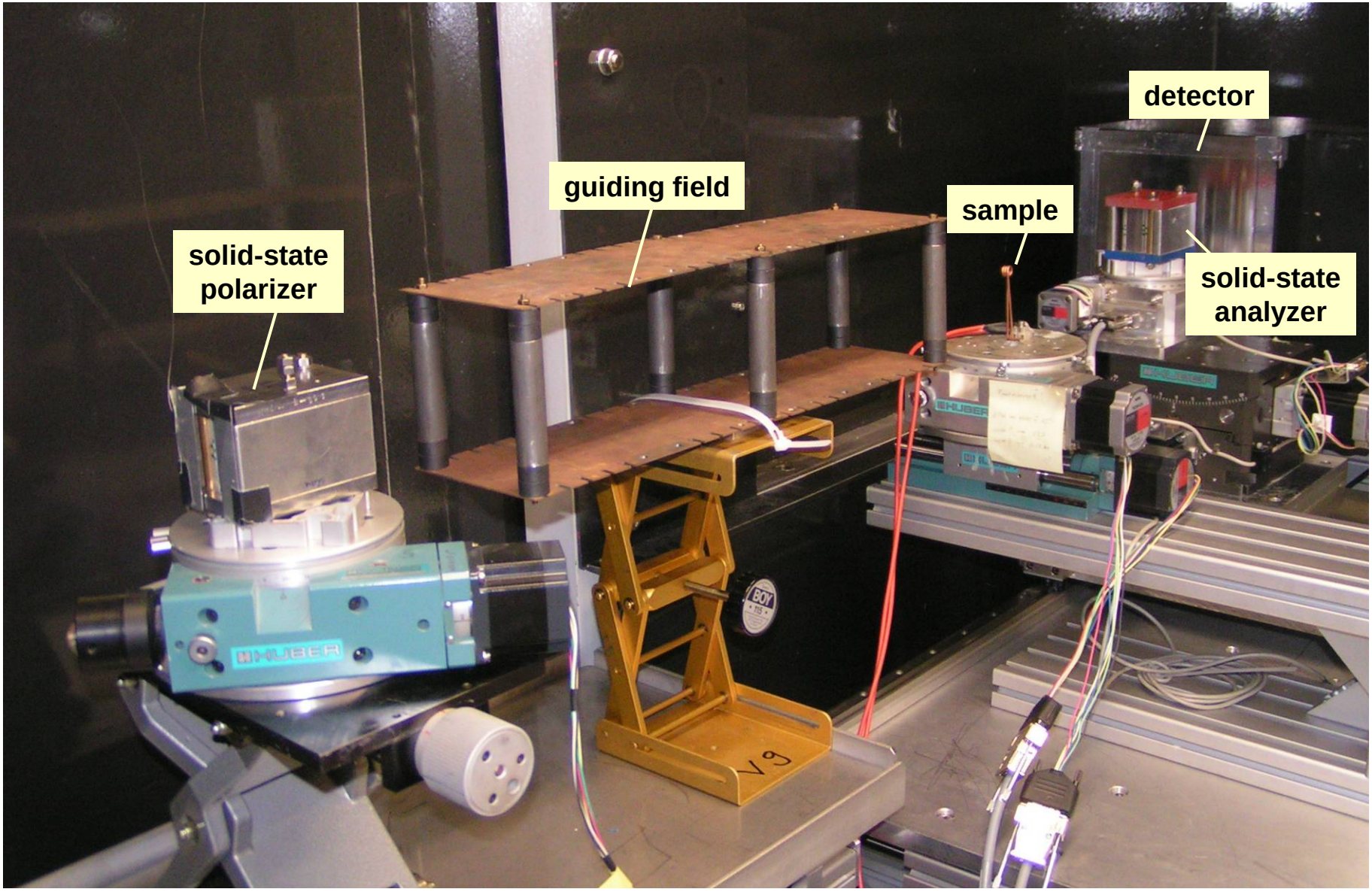

Imaging with polarized neutrons

Open beam (without sample)

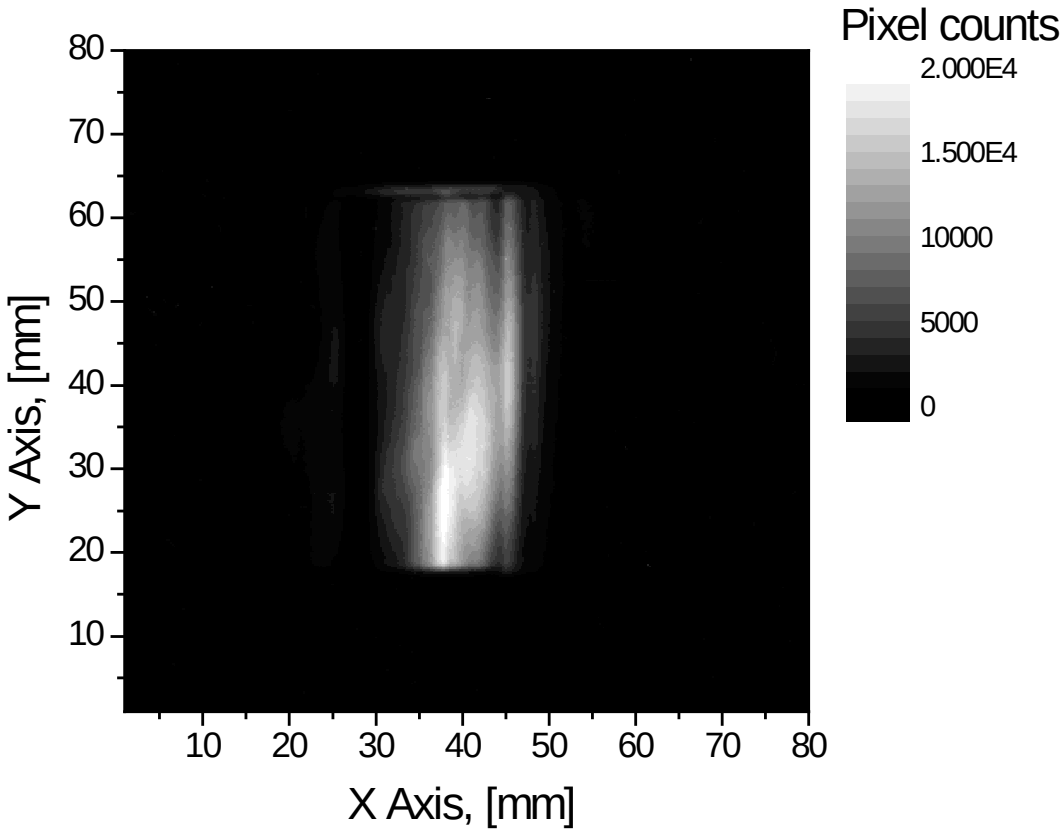

Exposure time: 300 s
Binning: 2x2

Sample

Copper coil
Wire thickness: 2 mm

Imaging with polarized neutrons

Radiography of magnetic field produced by a coper coil applying different currents using polarised neutrons

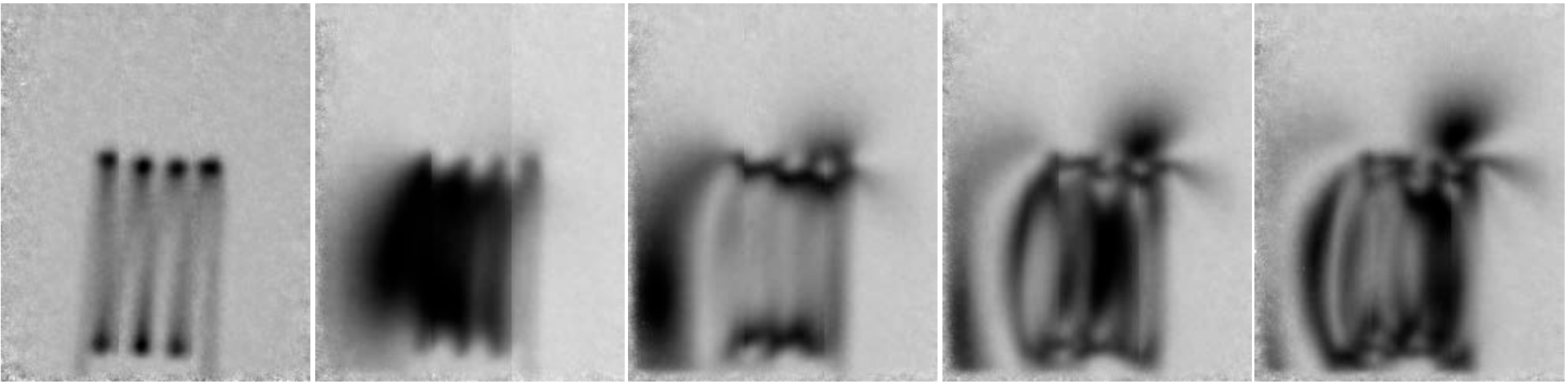

current: 0 Amp 4 Amp 8Amp 12 Amp 15 Amp

For the imaging setup, a polariser and analyser are used to convert the precession angle φ of the neutron spin after transmission through the magnetic to imaging contrast, respectively.

Imaging with polarized neutrons

Radiography of magnetic field produced by permanent magnets using polarised neutrons

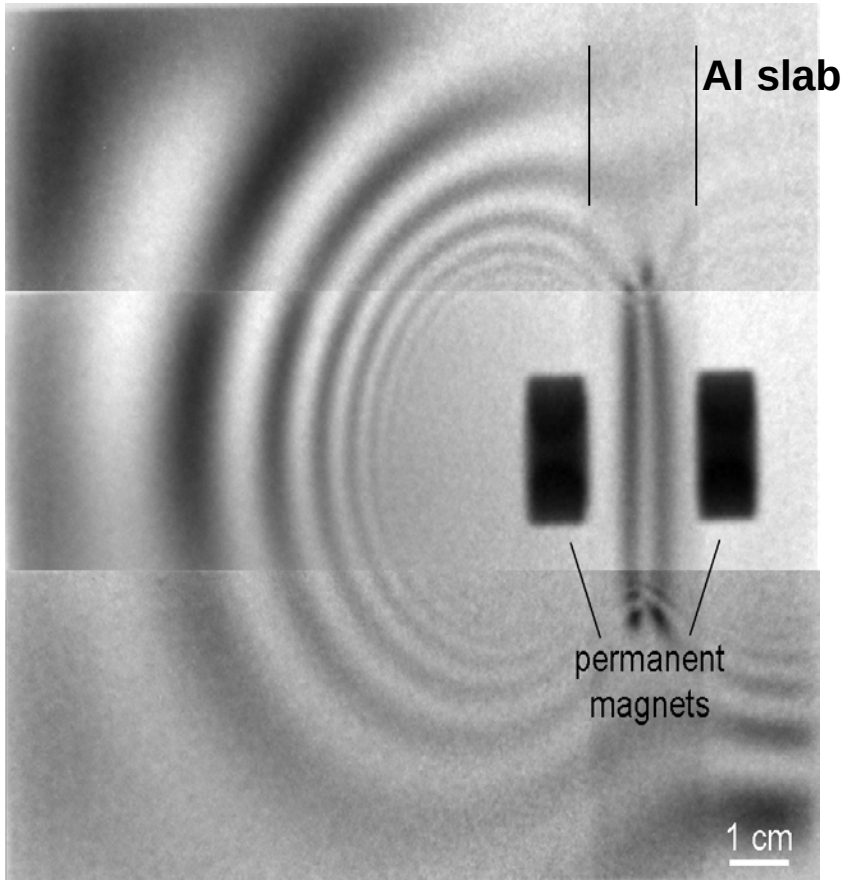

dipole magnets

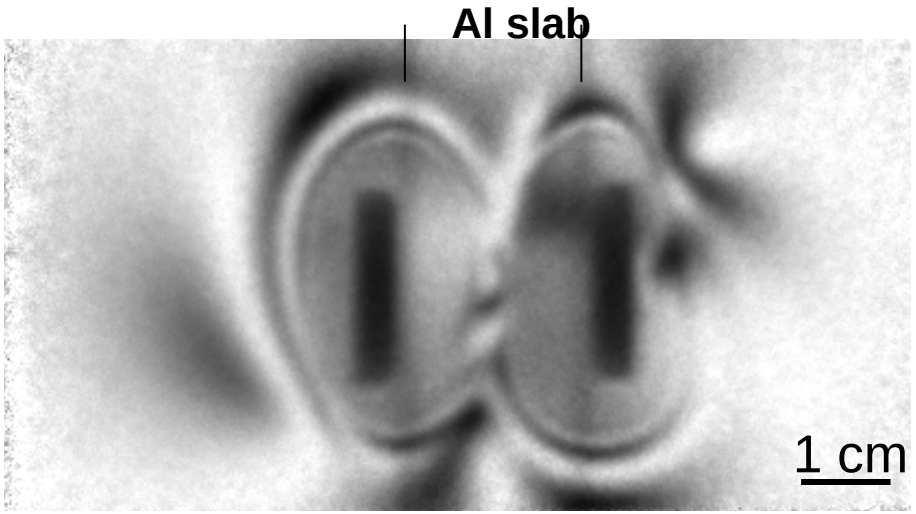

non-dipole magnets

Imaging with polarized neutrons

Simulations

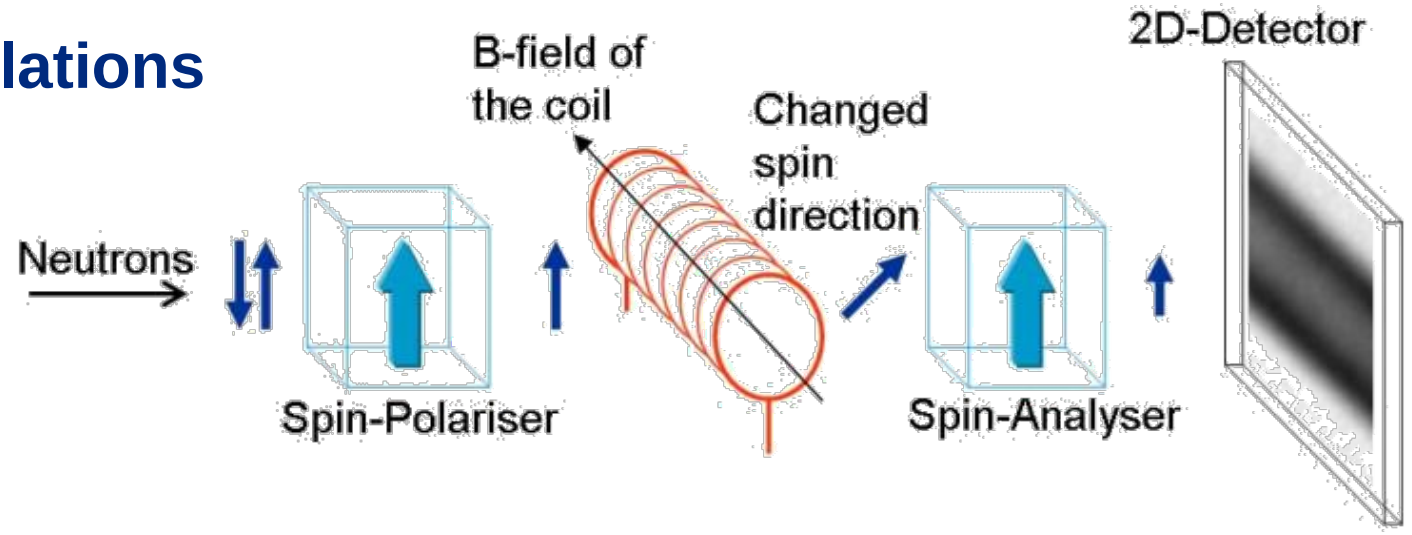

Biot-Savart law

$$d\vec{B} = \frac{\mu_0}{4\pi} \frac{I d\vec{l} \times \hat{r}}{r^3}$$

$$\phi = \frac{\gamma_L}{v} \int_{path} B ds$$

Spin rotation

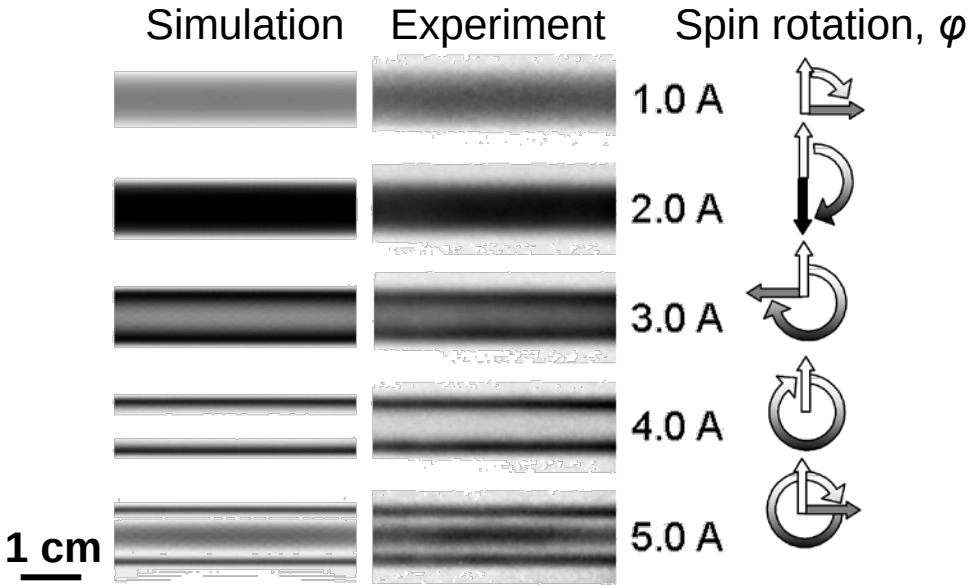

Simulation process - results

Double rectangle coil

- length = 36 mm
- width = 7 mm
- height = 21 mm
- windings = 30

- distance between the coils = 20 mm
- applied currents = 0.0 – 9.0 A
- field strength B = 1.05 mT @ I=1A

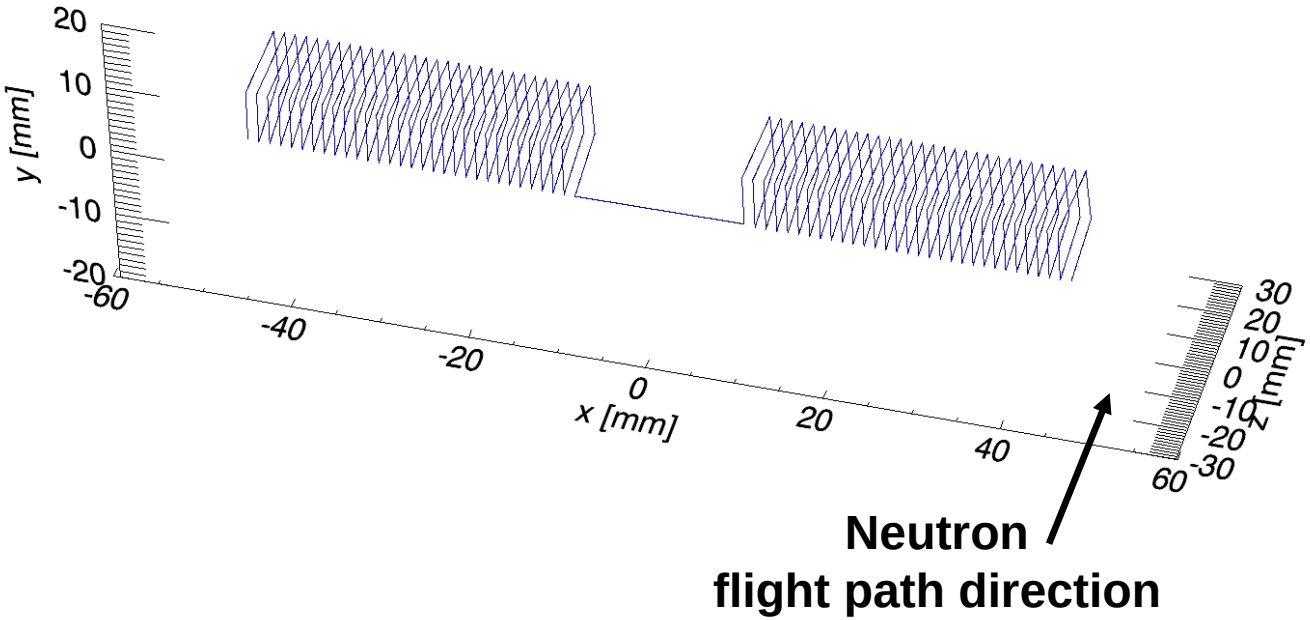

Simulation process - results

1.0 A

5.0 A

9.0 A

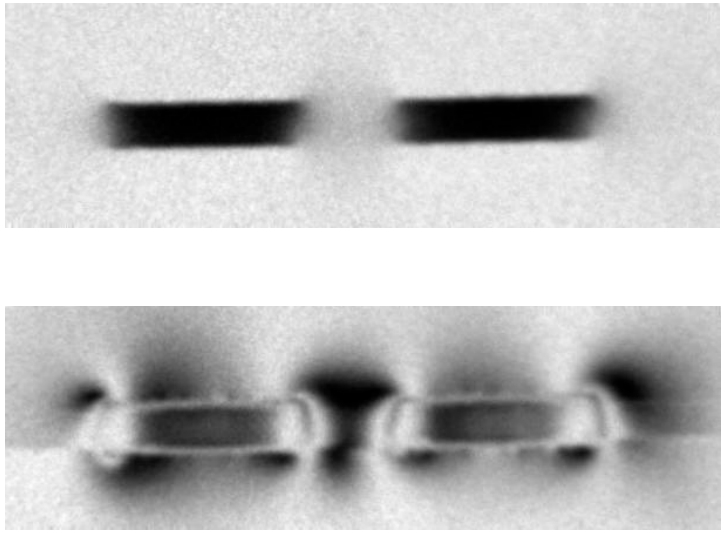

Simulated radiograms

Measurements

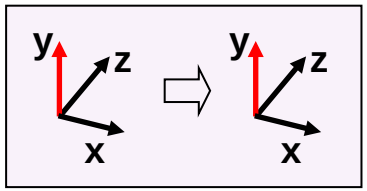

Application: Meissner-Effect

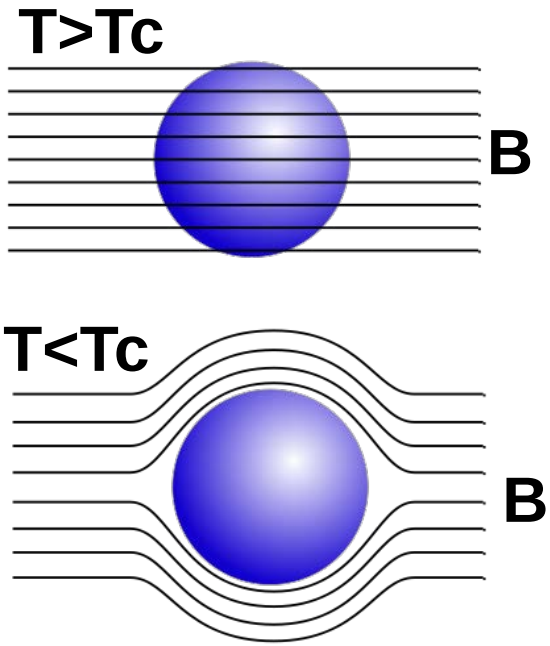

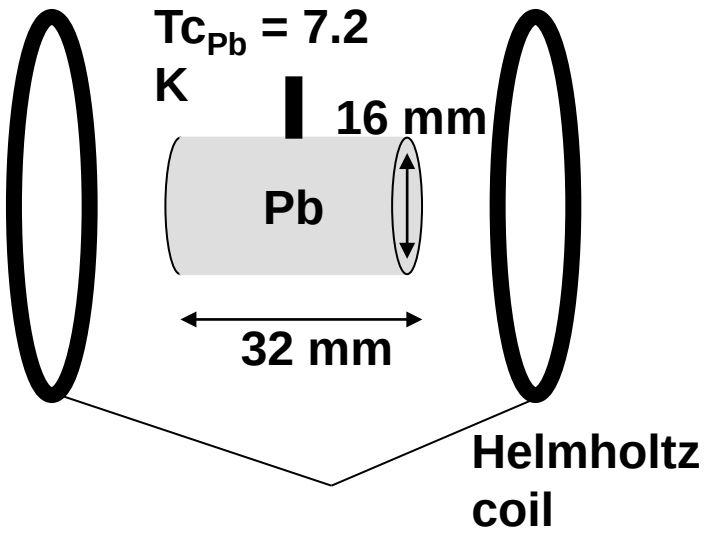

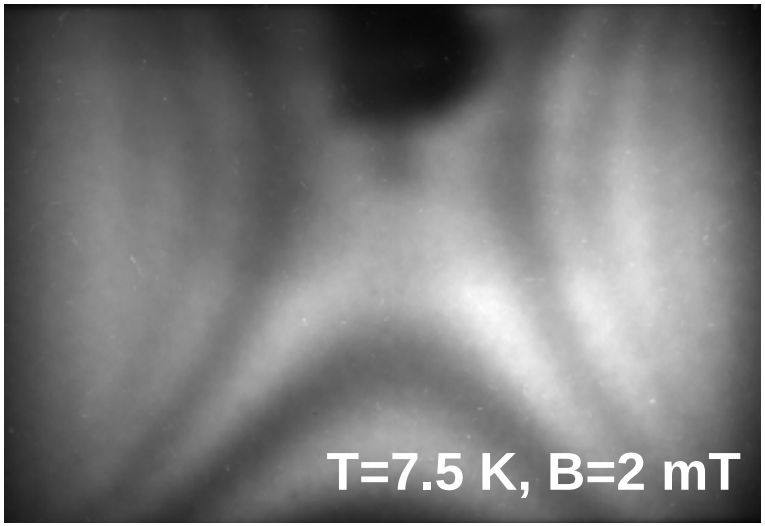

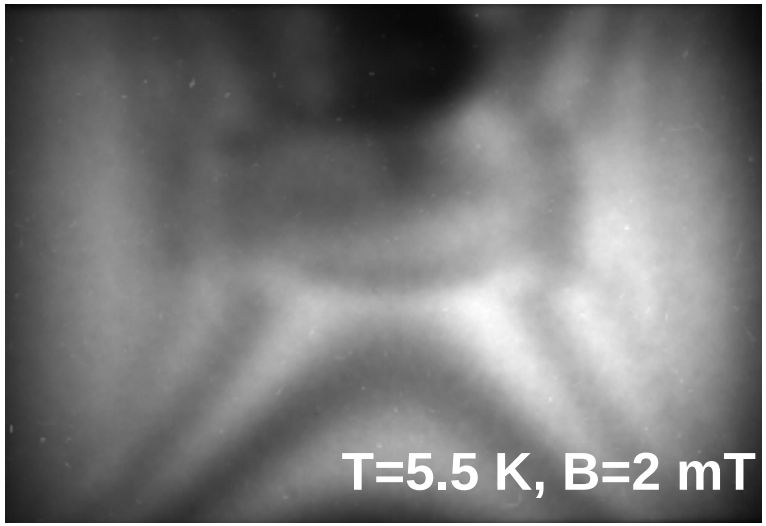

1 cm

Application: Meissner-Effect

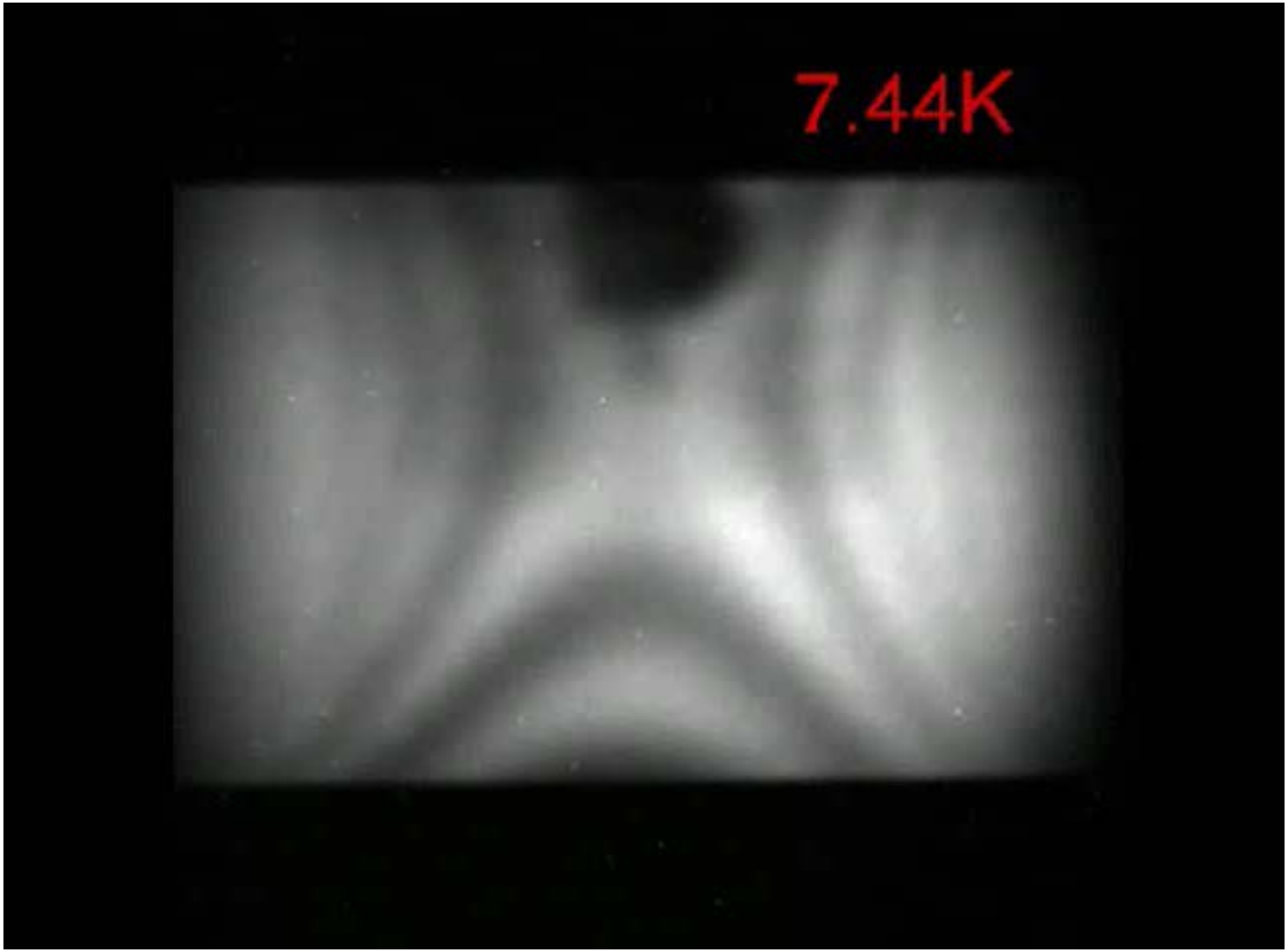

Magnetic Contrast

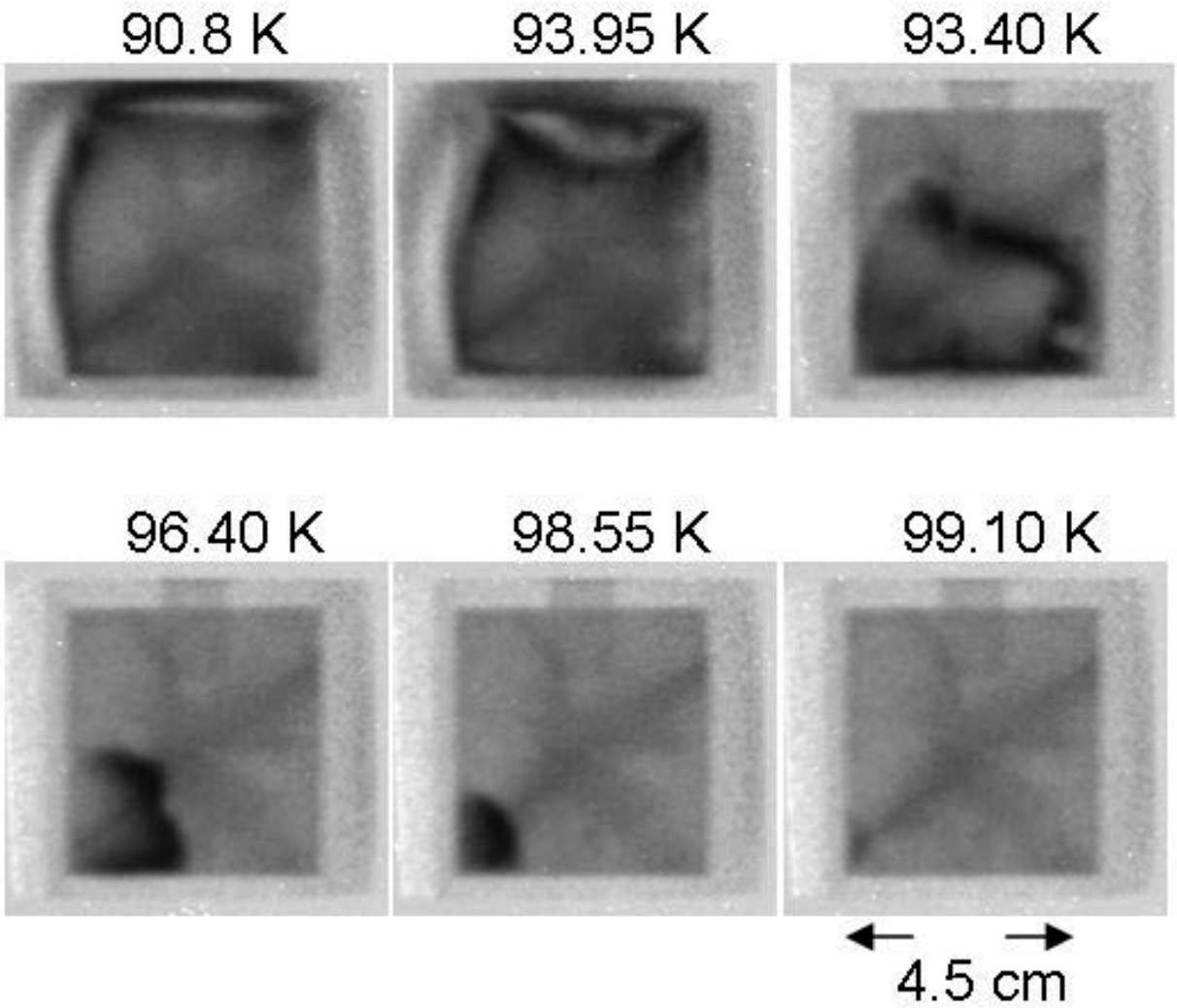

Flux trapping in a 45x45x12 mm^2 bulk YBCO sample.

Magnetic Contrast

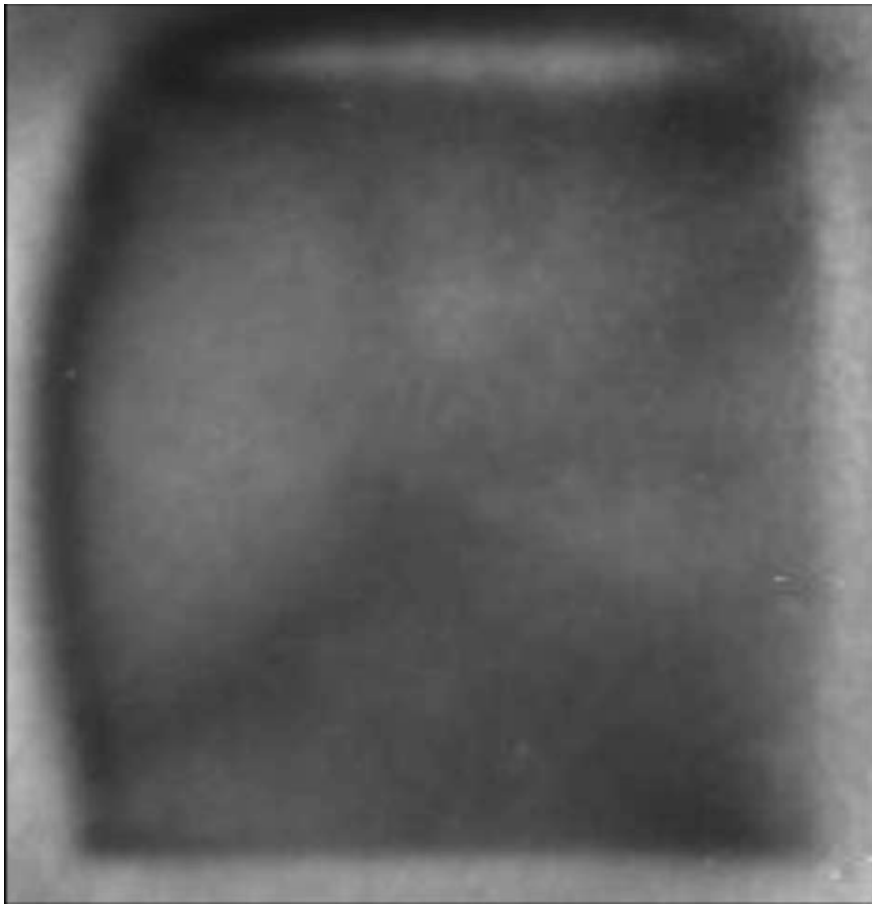

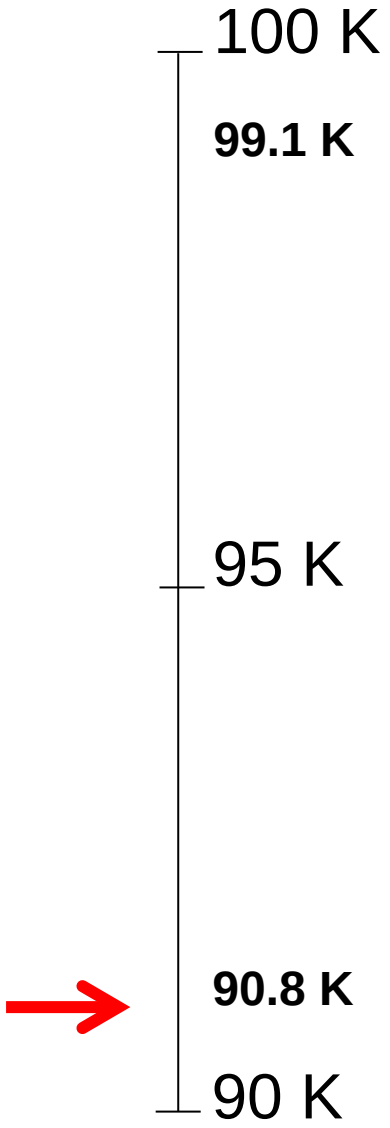

Flux trapping in a 45x45x12 mm² bulk YBCO sample.

Magnetic Contrast

Flux pinning in superconductors

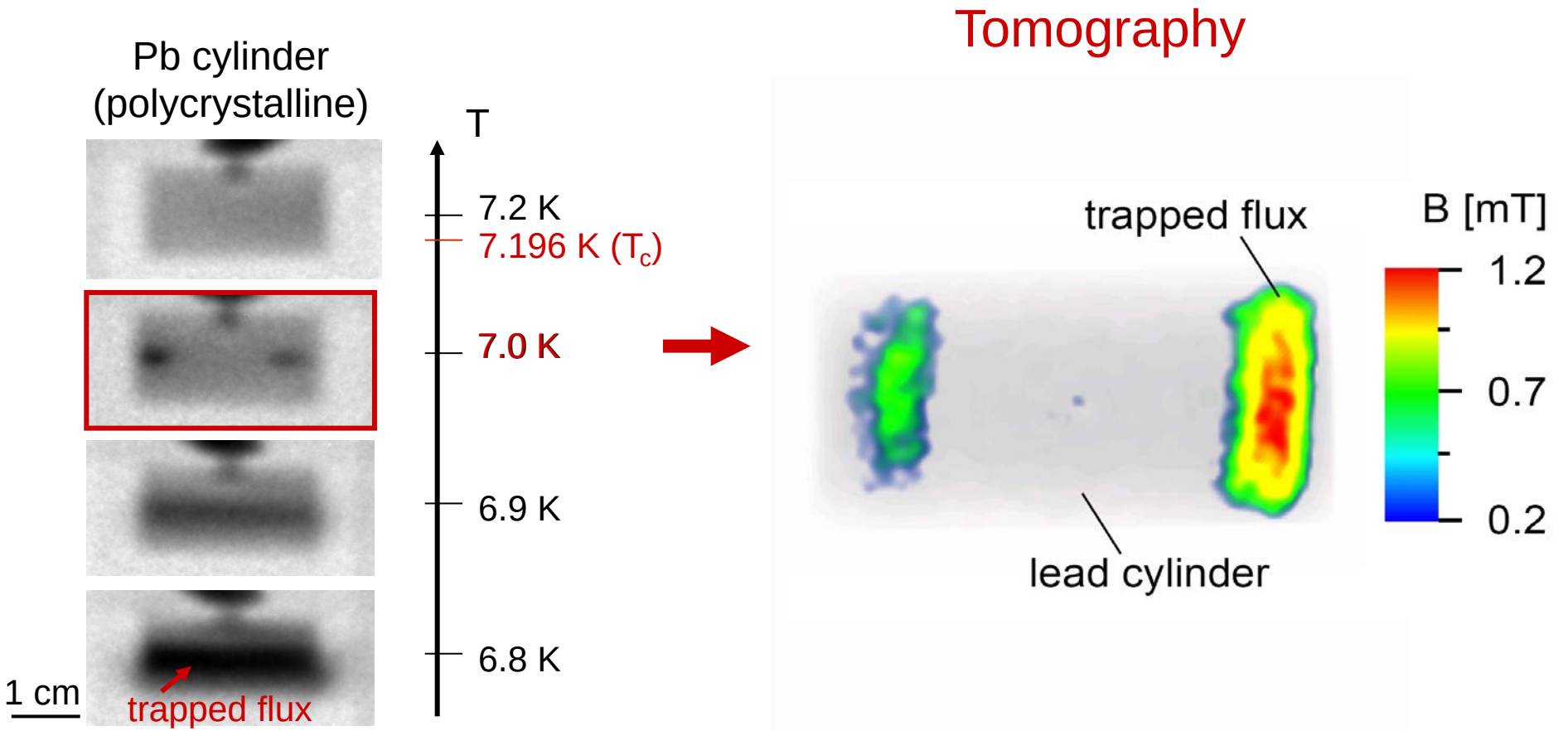

Flux pinning at cooling down below Tc while applying a homogenous magnetic field of 10 mT perpendicular to the beam.

The images were recorded after switching off the magnetic field.

N. Kardjilov, et al, Nature Physics 4, 399-403, (2008)

Imaging with polarized neutrons

Quantification of the magnetic field in 3D is another task that can be solved by using polarised neutrons.

The measurement of the precession angle for each of the three orthogonal spin components X, Y and Z provides a set of projections which allow for a tomographic reconstruction of the magnetic field produced by a sample.

The method is applicable for the visualisation of small magnetic fields (few mT) with a limited spatial resolution (500 µm).

M. Sales, et al., *Scientific reports* 8.1 (2018): 2214
A. Hilger, et al. Nature communications 9.1 (2018): 4023.

Imaging with polarized neutrons

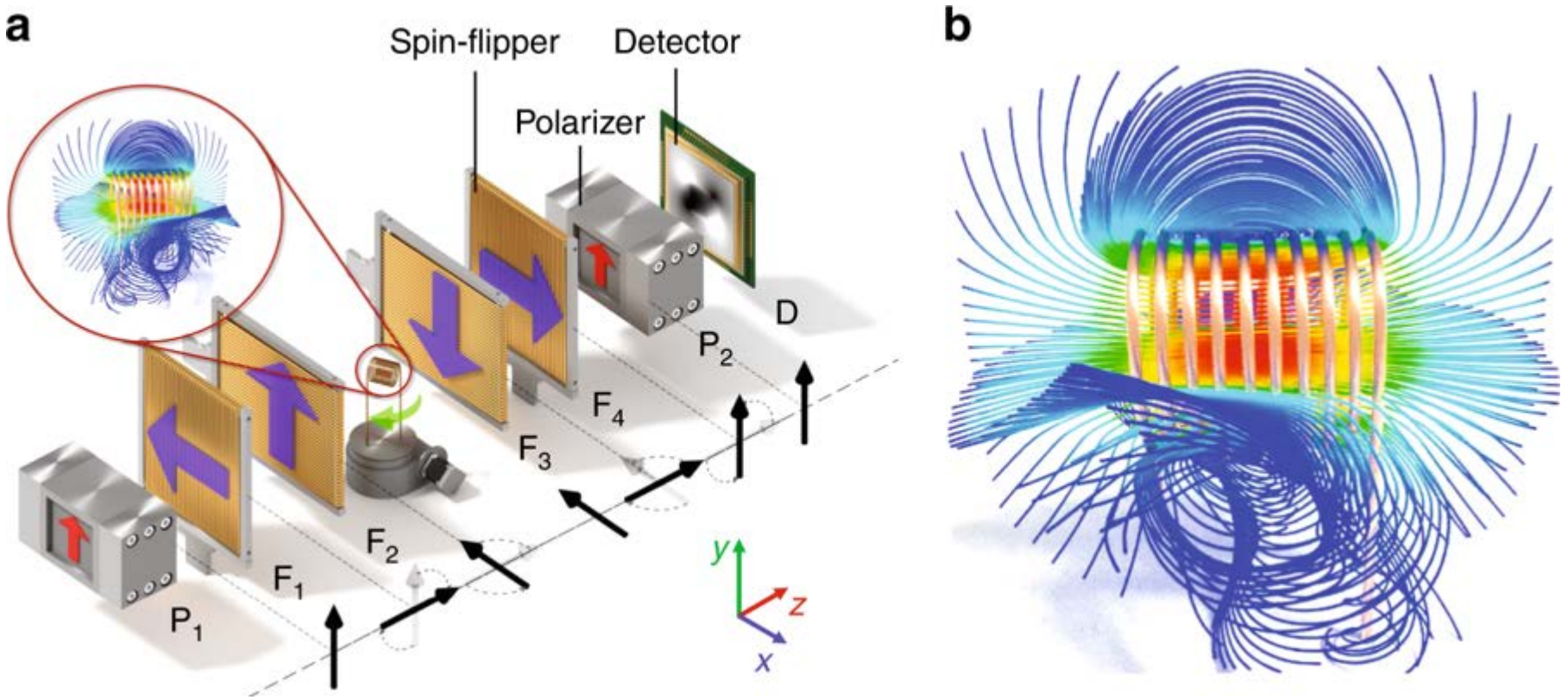

Tensor tomography. **a** Schematic drawing of the setup used for tensor tomography with spin-polarized neutrons, comprising spin polarizers (P), spin flippers (F) and a detector (D). **b** Selected magnetic field lines around an electric coil (calculation)

M. Sales, et al., *Scientific reports* 8.1 (2018): 2214
A. Hilger, et al. Nature communications 9.1 (2018): 4023.

Imaging with polarized neutrons

Comparison between calculation, simulation and measurement of the magnetic vector field produced by a sollenoid at 0.6 Amp.

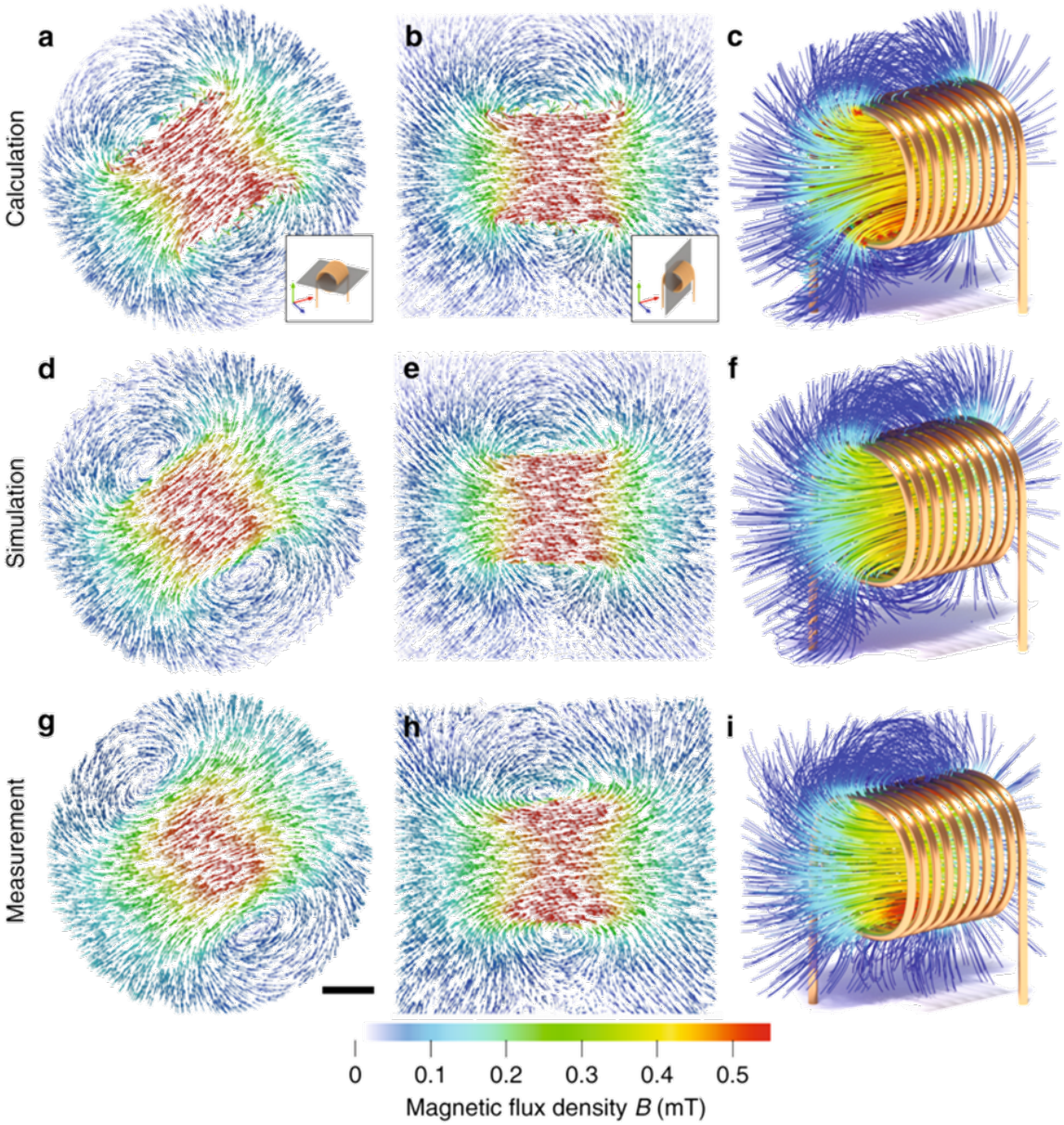

Quantitative magnetic tomography

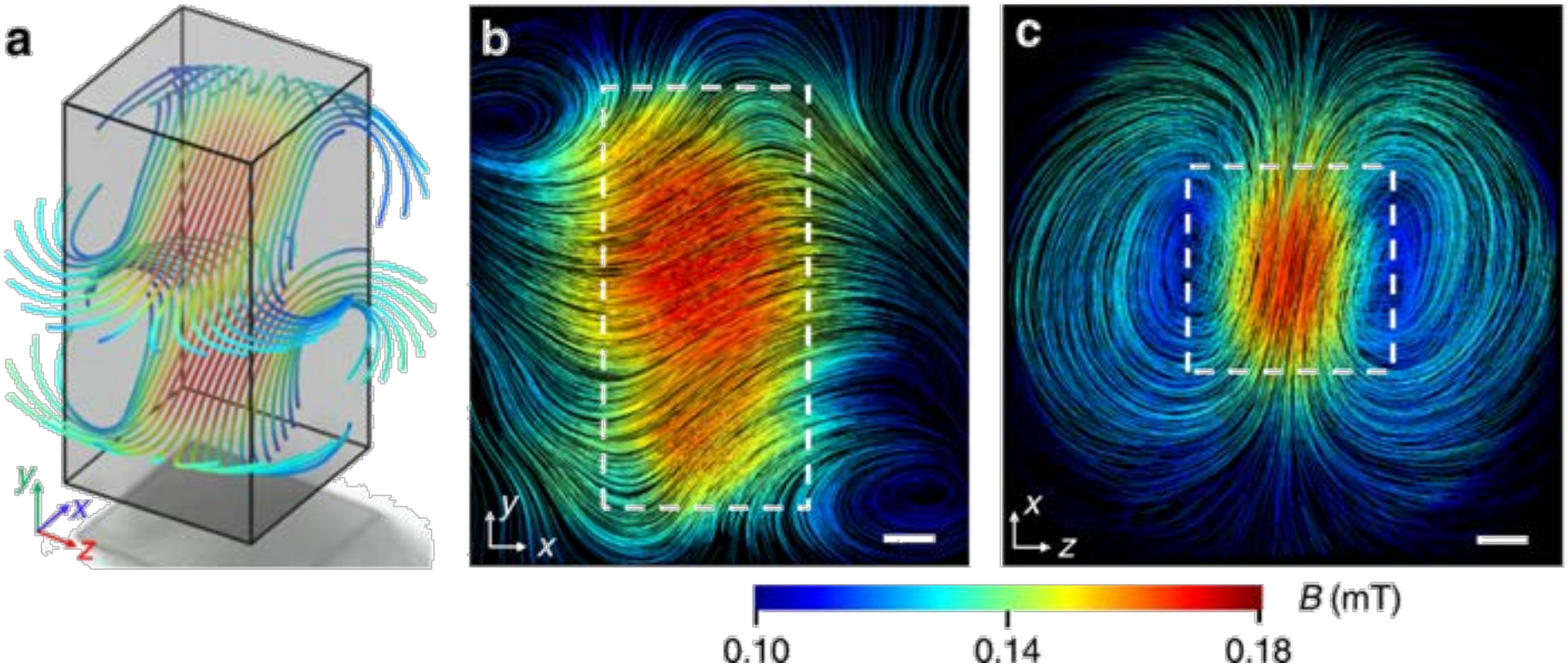

Magnetic vector field inside a superconducting lead sample measured at $T = 4.3$ K. **a)** Some selected magnetic field lines show the location of the magnetic field inside the sample indicated by the cuboid. **b)** Magnetic field lines in a selected *xy* plane (silhouette of the lead sample marked by dotted lines). Scale bar, 5 mm. **c)** Magnetic field lines in a selected *xz* plane. Scale bar, 5 mm.

A. Hilger, et al. Nature communications 9.1 (2018): 4023.

Application: Skin-Effect

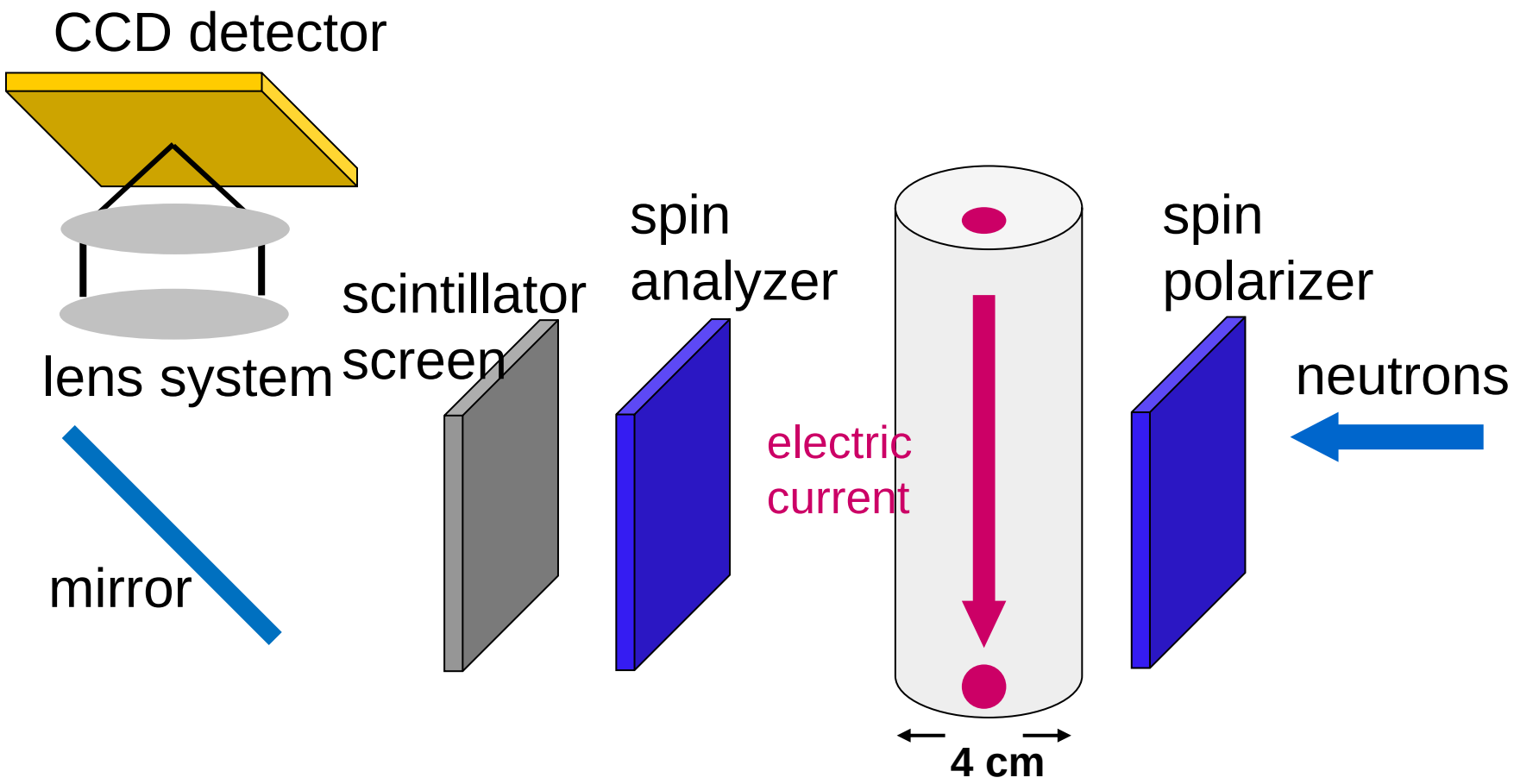

Manke, I., et al. *Journal of Applied Physics* 104.7 (2008): 076109-076109.

Application: Skin-Effect

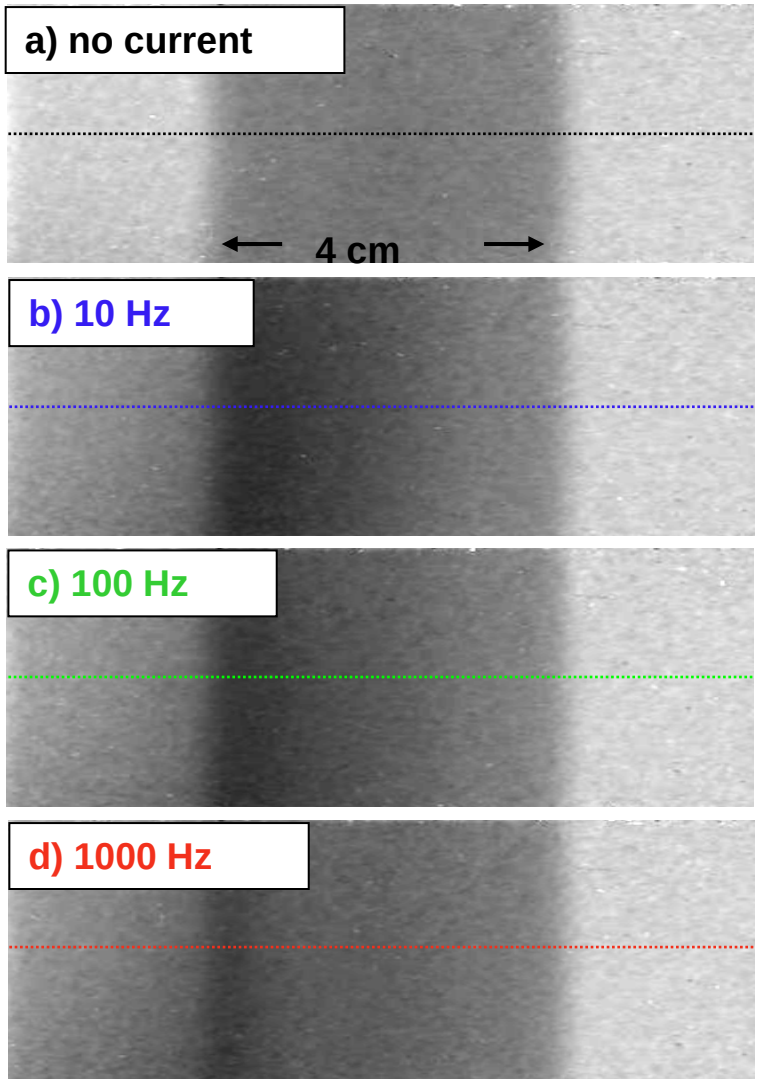

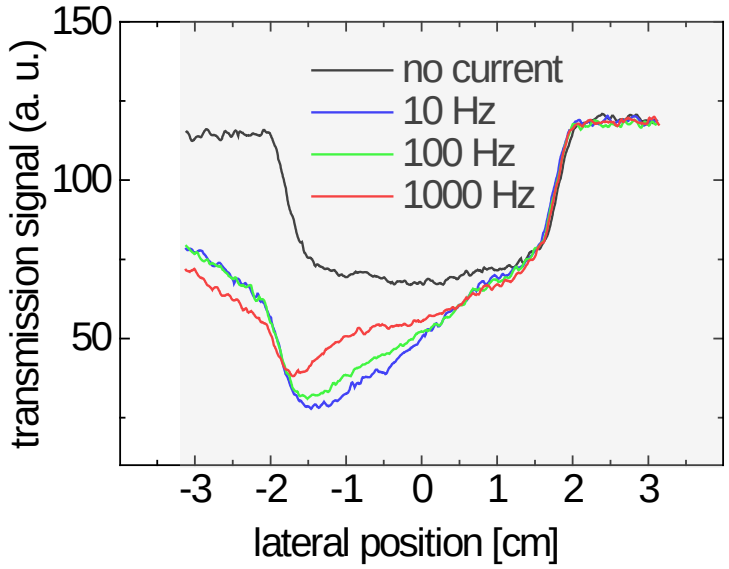

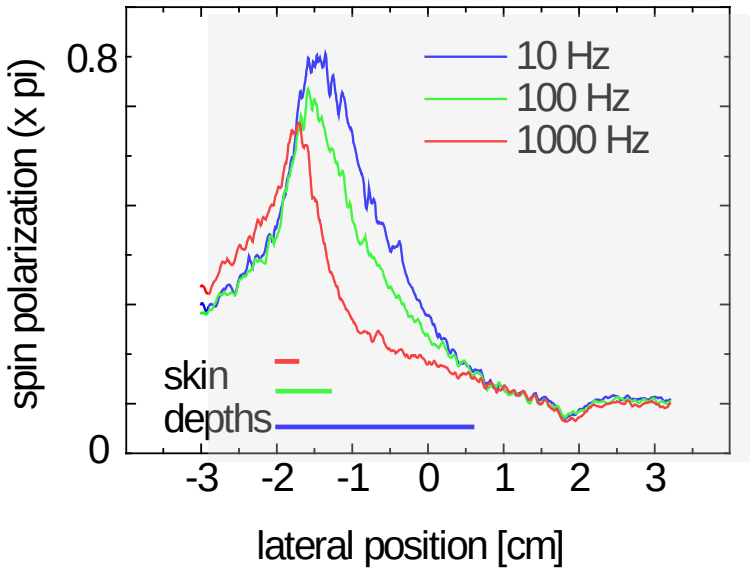

Manke, I., et al. *Journal of Applied Physics* 104.7 (2008): 076109-076109.

Magnetic Contrast

Depolarisation analysis

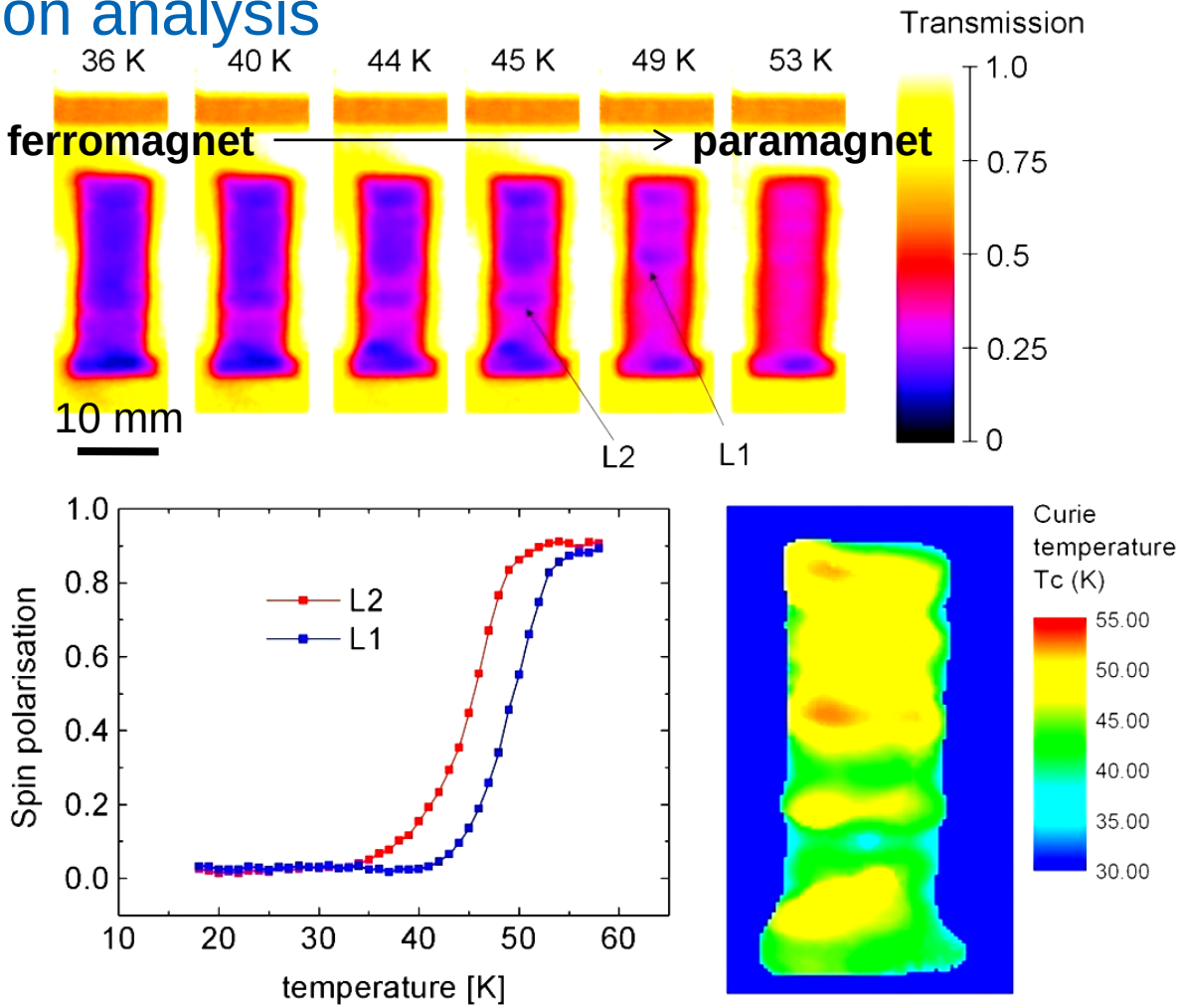

PdNi crystal (3.24% Ni) imaged by polarised neutrons

Thank you !

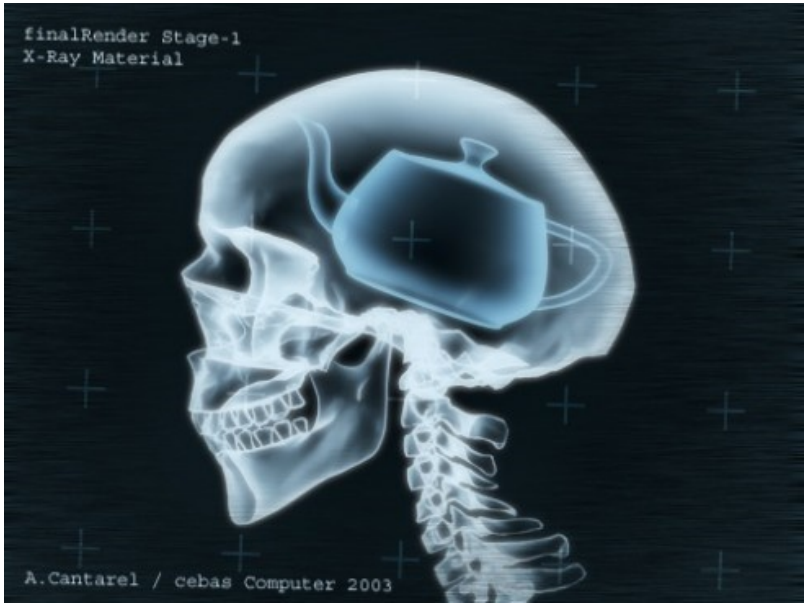
finalRender Stage-1
X-Ray Material
A.Cantarel / cebas Computer 2003